Controls on alluvial fan long-profiles

Jonathan D. Stock*
Kevin M. Schmidt
David M. Miller
U.S. Geological Survey, 345 Middlefield Road, Menlo Park, California 94025, USA

ABSTRACT

Water and debris flows exiting confined valleys have a tendency to deposit sediment on steep fans. On alluvial fans where water transport of gravel predominates, channel slopes tend to decrease downfan from ~0.10–0.04 to ~0.01 across wide ranges of climate and tectonism. Some have argued that this pattern reflects grain-size fining downfan such that higher threshold slopes are required just to entrain coarser particles in the waters of the upper fan, whereas lower slopes are required to entrain finer grains downfan (threshold hypothesis). An older hypothesis is that slope is adjusted to transport the supplied sediment load, which decreases downfan as deposition occurs (transport hypothesis). We have begun to test these hypotheses for alluvial fan long-profiles using detailed hydraulic and particle-size data in sediment transport models. On four alluvial fans in the western U.S., we find that channel hydraulic radiiare largely 0.5–0.9 m at fan heads, decreasing to 0.1–0.2 m at distal margins. We find that median gravel diameter does not change systematically along the upper 60%–80% of active fan channels as slope declines, so downstream gravel fining cannot explain most of the observed channel slope reduction. However, as slope declines, channel-bed sand cover increases systematically downfan from areal fractions of <20% above fan heads to distal fan values in excess of 70%. As a result, entrainment thresholds for bed material might decrease systematically downfan, leading to lower slopes. However, current models of this effect alone tend to underpredict downfan slope changes. This is likely due to off-channel gravel deposition. Calculations that match observed fan long-profiles require an exponential decline in gravel transport rate, so that on some fans approximately half of the load must be deposited off channel every ~0.20–1.4 km downfan. This leads us to hypothesize that some alluvial fan long-profiles are statements about the rate of overbank deposition of coarse particles downfan, a process for which there is currently no mechanistic theory.

*E-mail: jstock@usgs.gov

Keywords: alluvial fan, long-profile, Mojave Desert, sediment transport.

INTRODUCTION

Sediment exiting confined valleys in debris flows or entrained in floods commonly spreads laterally, forming fans (e.g., Fig. 1). Where the proportion of sediment transported by water traction is substantial, these fans are commonly called

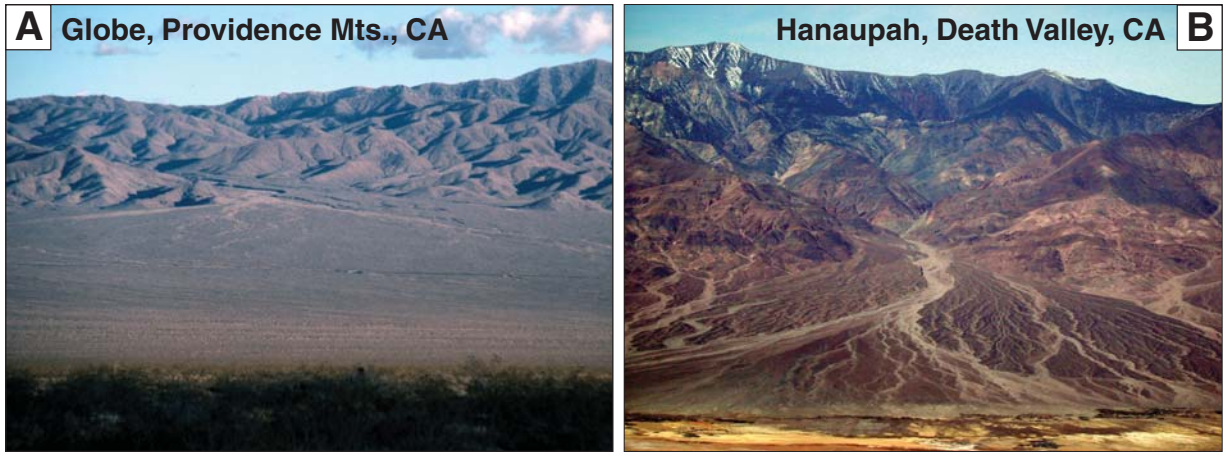

Figure 1. Photographs of alluvial fans whose modern channels transport gravel by water flow over a similar range of slopes. (A) Globe fan drains a low-relief (~500-m) source terrain of the Providence Mountains, eastern Mojave Desert. There are no active faults mapped in this area, and channel gradients decrease from ~0.06 at the active fan-head (high-albedo) channel to ~0.01, where the fan joins a sand-bedded axial wash. (B) Hanaupah fan drains a high-relief (~3000-m) source terrain of the Panamint Mountains, Death Valley, California. An active fault occurs in the lower right (see also Fig. 4), and fan gradients decrease from ~0.07 to less than 0.01, where the fan joins Badwater Playa in the foreground.

GSA Bulletin; May/June 2007; 120; no. 5/6; p. 619–640; doi: 10.1130/B26208.1; 23 figures; 4 tables.

alluvial, after Drew (1873). For alluvial fans with steep source catchments and traction-transported gravel, channel slopes commonly decrease from ~0.04–0.10 at fan heads to 0.01 or less at fan bases (e.g., Fig. 2). It is widely observed that deposits become increasingly fine grained downfan, from gravel-dominated proximal deposits, to sand-dominated distal deposits (e.g., Lawson, 1913; Eckis, 1928; Chawner, 1935). Average surface slope may vary down different azimuths (e.g., Hooke and Rohrer, 1977), but long-profiles are commonly concave up (e.g., Denny, 1965).

Drew (1873) proposed the first explanation for this concavity. He hypothesized that deposition reduced sediment supply progressively downfan. Consequently, the slope required to transport the supply of sediment decreased downfan (e.g., Fig. 3A). Concave-up long-profiles were, in part, a statement about the rate of downfan bed-material deposition. Later flume experiments (e.g., Ikeda and Iseya, 1988) have shown that Drew's hypothesis can be demonstrated in the laboratory, where flume channel slope decreased as gravel supply rate was reduced for a constant discharge. But this hypothesis was never tested on alluvial fans because subsequent work focused on the control of slope by grain size

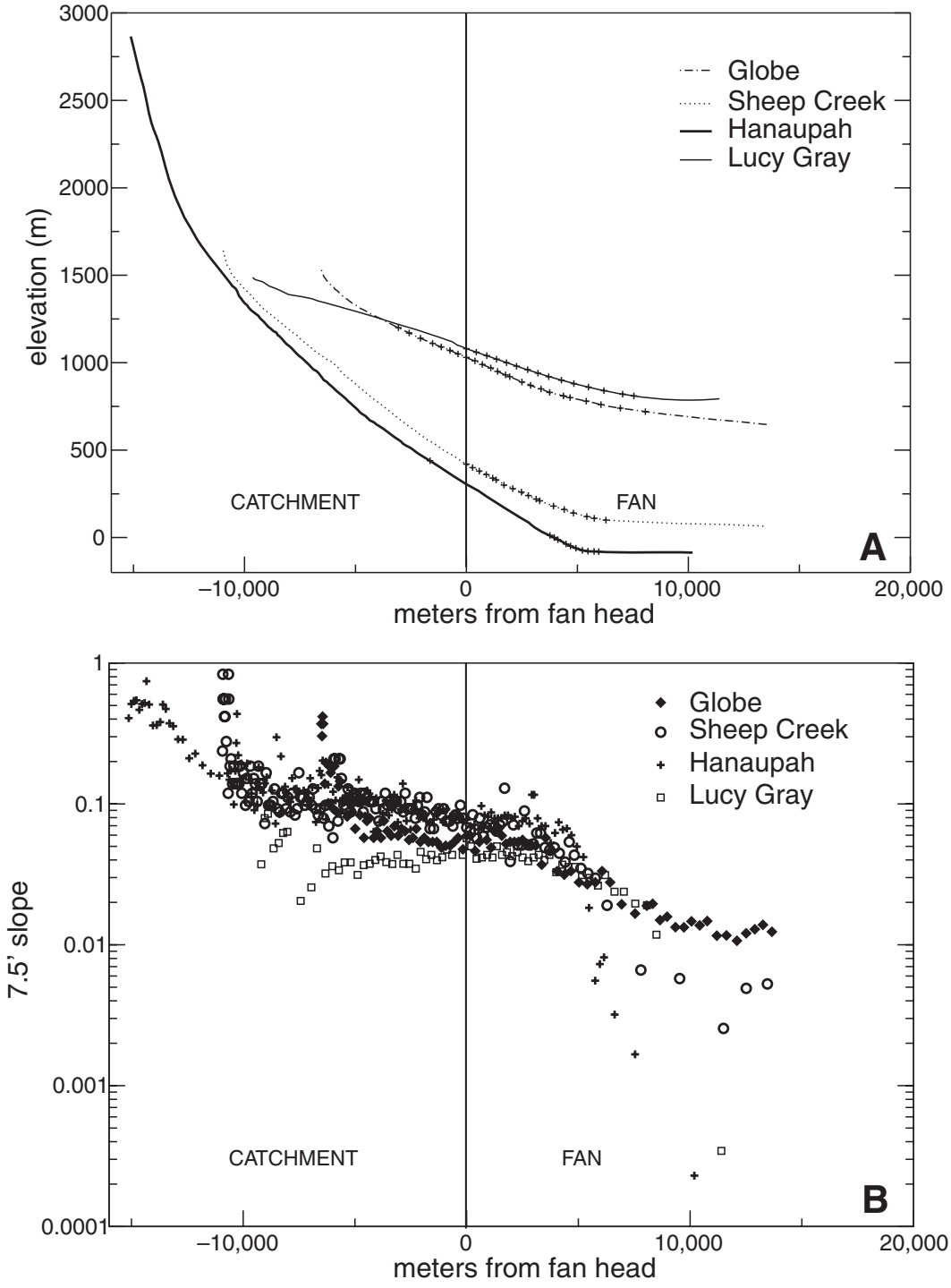

Figure 2. (A) Channel long-profiles down most active axial thread of four intensively studied fans and their source areas—Globe, Sheep Creek, Hanaupah, and Lucy Gray. Data extracted from U.S. Geological Survey 7.5′ topographic maps, starting at valley head (see Stock and Dietrich, 2003). Ticks indicate cross sections where we collected hydraulic geometry and grain size; endpoints approximate fan terminuses. (B) Slopes for each long-profile using every contour on U.S. Geological Survey 7.5′ topographic maps. We attempt to test whether this slope change is a statement about threshold sediment transport associated with downfan bed-material fining or sediment transport rates that decline downfan.

alone. Workers proposed that local slope is set by the coarsest grain fraction that can be entrained at a given reach (Fig. 3B); as this threshold grain size decreases downfan, fan slopes decline (e.g., Blissenbach, 1952, 1954; Bluck, 1964; Hooke, 1968; Kesel, 1985; Kesel and Lowe, 1987). In one of the most commonly cited examples, Blissenbach (1951, 1952, 1954) measured maximum clast size at cut banks down dissected fans of the Santa Catalina Mountains, Arizona. He reported a strong covariance between maximum clast size and local surface slope, an observation that has formed the basis for much subsequent work. This threshold hypothesis is widely accepted in the literature (McGowen, 1979; Nilsen, 1982; Ethridge, 1985; Miall, 1996) and has been used to model alluvial fans (Price, 1974).

These alternate hypotheses for downfan slope reduction can be restated (Fig. 3) as transport versus threshold entrainment controls on fan long-profiles. However, it is not clear which process dominates in the field, because despite over one hundred years of field work and modeling (summarized in Table 1; and by Bull, 1977; Nilsen, 1982; Blair and McPherson, 1994a, 1994b), the literature does not contain sufficient hydraulic and grain-size data to test these alternate hypotheses. Most studies (e.g., Eckis, 1928; Beaty, 1963; Bluck, 1964; Kesel, 1985; Kesel and Lowe, 1987; Hubert and Filipov, 1989) characterized grain size as the median or average of the coarsest ten grains within a given square or distance, sampling in straight lines downfan, potentially across deposits of different age and processes. This characterization creates two difficulties in using the data. First, it is difficult to isolate the role of individual processes. Second, there is no theory for the effect of exceptional grain sizes (e.g., maximum clast size) on channel reach slope. For instance, some flume studies (e.g., Solari and Parker, 2000) indicate that at slopes >0.02, the coarsest particles may be exceptionally mobile because of strong drag forces. As a result, the assumption underlying earlier studies that grain size controls slope cannot be tested with available data. Although it is known from photographs and field inspection that the grain size of many alluvial fans varies from gravel dominated to sand or finer fraction deposits at distal margins, data describing exceptional clast sizes are not a sufficient description to understand fan sediment entrainment or transport.

The same lack of data makes it difficult to evaluate recent theoretical models developed by Parker et al. (1998a, 1998b) and by Whipple et al. (1998). These studies used sediment transport models with thresholds to investigate long-profiles of tailing basin fans and, for the first time, explored Drew's hypothesis with a modern understanding of sediment transport. Under equilibrium conditions with channelized flow, constant grain size, and subsidence rate, these elegant models show that slope declines downfan as active channel width decreases and flow depth increases. Under these conditions, slope is proportional to the ratio of sediment to water discharge, a finding consistent with earlier experimental work by Hooke and Rohrer (1979). However, these models have not yet been tested on field-scale alluvial fans because of the lack of data.

In the following sections, we describe field sites, methods, and models that we use in an attempt to test two alternate hypotheses for fan long-profiles (Fig. 3) in four gravel-dominated

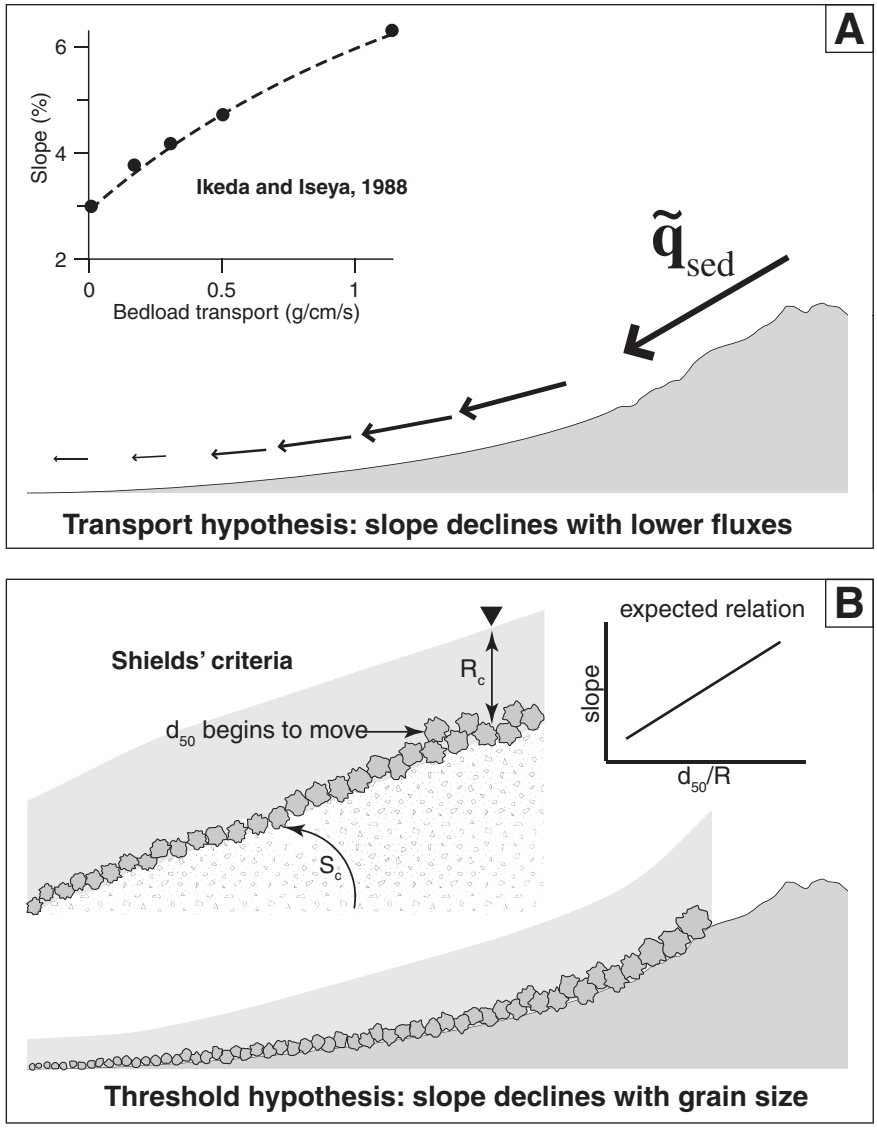

Figure 3. Conceptual model of factors that control alluvial-fan slope. Figure 3A illustrates Drew's 1873 hypothesis that declining transport rate q_{sed} (decreasing arrows) downfan lead to slope reduction (long-profile modified from Drew, 1873). Inset graph modified from Ikeda and Iseya (1988) illustrates this effect in a supercritical flume whose slopes approximate those found on many alluvial fans (e.g., Fig. 2B). Figure 3B illustrates later threshold hypothesis (e.g., Blissenbach, 1952) that declining grain size downfan (either because of shallowing flow, as shown, or because of comminution) leads to a decrease in slope. Inset shows an illustration of this effect as characterized by Shields' criterion (see Equation (1) in text), where particles of d_{50} diameter begin to move once flow reaches a depth of R_c at S_c slope. Smaller inset shows predicted relation between channel slope and ratio of d_{50} to R for a threshold entrainment channel.

TABLE 1. SUMMARY OF HYDRAULIC, SEDIMENTOLOGIC, AND MORPHOMETRIC OBSERVATIONS ON ALLUVIAL FANS

Observation	Variable/equation	Interpretation/generalization	Location	Example reference(s)
Hydraulic and sedimentologic				
Standing waves	$1.1 < Fr < 2.1$	Flow near critical or supercritical	Southwest Arizona	Rahn, 1967
Standing waves; $F_r > 0.7$	$1.3 < Fr < 2.0$	Flow near critical or supercritical	Death Valley, California	Beaumont and Oberlander, 1971
Standing waves (antidunes?)	$Fr > 0.7$[?]	Flow near critical or supercritical	Roaring River, Colorado	Blair, 1987
Channel thread inundated			Central America; Arizona	Kesel, 1985; Pearthree et al., 2004
Some runoff sourced on fan		Pedogenesis affects hydraulics?	Western U.S.	Denny, 1965, 1967; Beaty, 1968
Moved particle diameter ~ flow depth		Drag forces predominate?	Death Valley, California	Beaumont and Oberlander, 1971
Maximum grain size fines downfan		Maximum grain size controls slope	Western U.S./ Central America	Eckis, 1928; Chawner, 1935; Blissenbach, 1952; Beaty, 1963; Bluck, 1964; Kesel, 1985; Ritter et al., 1993
Grain size may show no pattern		Influence of debris flows/tectonics Source grain size limitation	Western U.S.	Bull, 1964a; Lustig, 1965; Denny, 1965; French and Lombardo, 1984; Wells, 1977; Hubert and Filipov, 1989; Ritter et al., 1993; Blair, 1999, 2000; Mather and Hartley, 2005
Sand fraction (weight) increases downfan		Rapid gravel deposition?	Death Valley, California	Blair, 2000
Channel widens with increase in sediment supply/discharge		Width adjusted to sediment discharge?	Central America; Arizona	Kesel, 1985; Field, 2001
Downfan channel hydraulic geometry (width, depth, slope)		–	None	None found
Bedload flux		–	None	None found
Morphometric				
Fan depositional area is power function of source area	$A_{fan} = cA_{drainage}$	Sediment yield controls fan area; artifactual covariation with drainage spacing & lower b.c.?	Western U.S./Persia Canada/Spain	Bull, 1962; Bull, 1964b; Denny, 1967; Hooke, 1968; Beaumont, 1972; Kostaschuk et al., 1986; Harvey, 2002
Fan channel width increases with $A_{drainage}$	$W_{fanchannel} = cA_{drain.}$	Width adjusted to water & sediment discharge	Western U.S.	Denny, 1965; Wells, 1977; Harvey, 1987
Fan slope decreases with $A_{drainage}$	$S_{avg} = cA^{n}$	Artifactual from concave up long-profiles?	Himalaya/western U.S. Central America/Spain	Drew, 1873; Eckis, 1928; Bull, 1962; Melton, 1965; Kesel, 1985; Harvey, 1987; Harvey, 2002
Fan slope increases with relief of source basin	$S_{avg} = 7.3(H/A^{0.5})^{0.87}$	Influence of debris flows; long-profile concavity?	Arizona/Canada/Italy	Melton, 1965; Kostaschuk et al., 1986; Marchi et al., 1993
Slope increases with D_{max}		Artifactual covariation with slope?	Western U.S./ Central America	Blissenbach, 1952; Bluck, 1964; Kesel, 1985; Hooke and Rohrer, 1979
Slope independent of D_{max}		Slope not dependant on exceptional clasts?	Western U.S. Persia	Lustig, 1965; Boothroyd and Nummedal, 1978; Beaumont, 1972; Mills, 2000
Fan slope steepest off of main axis		Transport less frequent off-axis?	Western U.S.	Hooke and Roher, 1979

Note: ?—indicates our hypothesis to explain observation
[?]Minimum Fr number, author reports a range of 1.6 to 2.2 in text.

fans in the arid southwest USA (Fig. 4). These fans are characterized by steep source catchments with hillslope, debris flow, and fluvial processes that supply a wide range of grain sizes to fan heads, and ephemeral flow and sediment transport by traction (flowing water) in fan channels. We focus on channelized alluvial fans, whose high-albedo threads (e.g., Figs. 1 and 4) represent focused sediment transport down channels, not sector inundation and sheetflooding that may occur on some fans (e.g., Blair, 2000). We measure grain size and channel hydraulic geometry down active channel threads to test two proposed hypotheses for fan-channel slope changes. For instance, Shields' bed-material threshold entrainment model predicts that channel slope should increase as bed material becomes coarser for a given hydraulic radius. We test this statement of the threshold hypothesis by measuring fan-channel slope, hydraulic radius, and bed-material diameter to see whether they follow Shields' prediction for a threshold channel (Fig. 3B, upper right inset). A rigorous test of Drew's transport hypothesis would compare measured unit bedload flux down a fan sector to that predicted by a transport equation with field data inputs. For the moment, sediment flux measurements are too difficult to make in ephemeral channels. So, we use a less rigorous test and apply the field data to plot the unit bedload flux predicted by transport equations downfan, to see if this model is consistent with a reduction in bedload flux. The tests are applied to active fan channels with the understanding that departures from these conditions in the past could also influence fan surface slope. So, our analyses are strictly tests of these alternate threshold and transport hypotheses on modern fan channels that are presumed to be in equilibrium.

FIELD SITES

We selected four alluvial fans (Fig. 4; Table 2) in or near the Mojave Desert, California. Channel long-profiles for these fans (Fig. 2A) are concave up, and slope declines from ~0.04–0.09 at fan heads, to 0.01–0.005 at axial washes, and to negligible values at playa boundaries (Fig. 2B). The fans have radial form and active channel threads with plane bed or low-relief alternate bar and mid-channel bar morphology. Work by Pearthree et al. (2004), Vincent et al. (2004), and Pelletier et al. (2005) has shown that flow in such settings is focused into narrow threads, with deposition common in overbank areas, where unconfined flow may be referred to as sheetflooding.

Bedforms in these channels are composed of imbricated material transported by water traction. We identified deposits from traction transport (which could include hyperconcentrated

flow) using the following criteria: clast supported deposits and imbrication at both large and fine gravel fractions (pervasive imbrication). Although coarse particles in debris-flow levees and snouts can be imbricated (e.g., Major and Iverson, 1998), we have observed that finer grains in their interior lack pervasive imbrication. We identified debris-flow deposits in catchments above fan heads using criteria based on analysis of historic deposits (e.g., Costa, 1984; Stock and Dietrich, 2003): matrix supported clasts and a lack of pervasive imbrication at all grain scales.

Each fan also has a series of older alluvial deposits within which the modern active channels are inset. For this reason, flow and sediment transport are necessarily focused in narrow threads, and large amounts of sediment cannot have been deposited in modern channel beds since abandonment of these older surfaces. This timescale is important because it limits the time over which the boundary conditions on the fan (e.g., sediment supply rates, reach slope) can be considered relatively steady. The relative age of these older fan deposits can be inferred from pedogenesis and surface characteristics, which generally covary with elevation above the modern channel. Yount et al. (1994) established three main, time-based divisions for alluvial deposits—young, intermediate, and old. Briefly, we review the evidence for the age of these deposits, following Miller et al., 2008.

In the Globe fan area, active alluvial channels and adjacent sandy bars or terraces that are episodically inundated by overbank flow are the two youngest subdivisions of the young category. These deposits lack desert pavements and rock varnish, have a relatively high albedo in aerial photographs (e.g., Fig. 4), and have been active since the oldest wagon roads were established in this area, ca. 1–2 centuries ago. Older young alluvial fan deposits form adjacent, higher surfaces that only rarely show evidence for recent flood inundation and have denser vegetation including creosote bush, white bursage, cryptogamic mats, and annual grasses. These deposits display very weak pavements in some cases, slight varnish, weak vesicular A (Av) horizons, and weak cambic horizons (Bw). The oldest of the young category of deposits have noticeable desert pavements that do not interlock and whose pebbles are varnished and possess rubification (reddening). Underlying Av and Bw horizons are persistent features, with calcic morphology of stage I. Deposits of this category are darker toned on aerial photography than the next younger category, due to increased rock varnish and decreased plant cover. The young deposits occupy the bulk of the lighter areas in Figure 4. Luminescence, radiocarbon, and U-Th dates (e.g., Clarke, 1994; McDonald, 1994; Wang et al., 1994; Mahan et al., 2007; Sohn et al., 2007) indicate latest Pleistocene to Holocene deposition times for similar deposits.

Intermediate age deposits display desert pavement with interlocking, varnished surface clasts overlying a platy-structured Av horizon composed primarily of silt. The varnish creates the low albedo that characterizes much of the deposit in the images of Figure 4. Varying amounts of red to brown clay accumulation and iron oxidation yield a Bt argillic horizon. The calcic horizon typically is stage II to stage III (Gile et al., 1966; Machette, 1985). Most deposits with desert pavements have been dated as late Pleistocene, with some falling in the range of late-middle Pleistocene (Bull, 1991; Wang et al., 1994; Sowers et al., 1988; Mahan et al., 2007; Maher et al., 2007; Sohn et al., 2007).

Deposits classified as old alluvial fan deposits form linear ridges (whalebacks) whose rounded lateral margins indicate substantial erosion (Peterson, 1981). Remaining soil horizons are primarily the stage IV calcic horizon (e.g., Gile et al., 1966; Machette, 1985) and thin, degraded argillic horizons (e.g., Yount et al., 1994). Because petrocalcic material is present at the surface, these features may have high albedo. The 0.74-Ma Bishop ash is the most diagnostic tephra layer observed regionally in these old deposits (McDonald, 1994).

Globe

Globe fan (Figs. 1 and 4–7) carries sediment from low-relief (<500 m) headwaters cut largely in Proterozoic gneisses and Mesozoic granite. No Quaternary faults are known in either source area or fan. Field observations revealed that Holocene debris-flow deposits terminate at valley slopes of ~0.10, high above the fan head. Strongly indurated fanglomerates overlying gneiss are exposed in the channel thalweg just upslope from the fan head (near A in Fig. 5), indicating that the Globe channel here has not incised bedrock over late Pleistocene to Holocene time. High-fill terraces at the fan head display inconsistent pedogenesis and thin sheets of varying ages of alluvium as young as the oldest young deposits (latest Pleistocene). These relations indicate that fan head was episodically deposited over a long period of Pleistocene time and was dramatically incised in early young alluvial deposit time. Channels of the lower fan are disrupted by engineering berms meant to divert and concentrate flow under railroad bridges. These channels subsequently feed Kelso Valley axial wash, an ~0.01 slope, braided sand channel.

TABLE 2. FIELD SITES

Fieldsite	Range	State	Bounding fault	Max. source area relief (m)	DEM slope Mean (std. dev)	Fan head area (km^2)	Fan area# (km^2)	Arc length‡ (m)	Fan relief* (top)-(bottom) = (m)	Fan head slope (7.5′)	Average rain (mm/a)	Station′/ record length	Dominant lithologies	Reference(s)
Globe	Providence	California	inactive?	586	.41 (.18)	12.39	9.7/17.1	6500	1040 - 710 = 330	0.060	274	045721/ 1958-2005	Adamellite, gneiss, granite	Goldfarb et al., 1988
Lucy Gray	Lucy Gray	Nevada/ California	inactive?	1043	.33 (.19)	44.29	64.9	8200	1090 - 800 = 290	0.057	214	045890/ 1955-2005	Granitoids, volcanics	Hewett, 1956
Sheep Creek	Avawatz	California	thrust	1444	.52 (.21)	20.60	20.2/22.3	5800	430 - 110 = 320	0.068	69	040437/ 1953-1971	Gneiss, granitics, metavolcanics	Brady, 1986
Hanuapah	Panamint	California	Normal?	3055	.57 (.20)	74.05	16.0/45.3	5800	256 - (-82) = 338	0.062	58	042319/ 1961-2005	Argillite, dolomite, granite, qtzite	Albee et al., 1981

?From 1-m (Globe) or 10-m DEM of catchment above fan head.
#Approximated using DOQQ.
‡Straight line from fan head to margin along central axis. Second area is for pre-Holocene far area shown in Figure 4.
*Fan head contour minus margin contour.
′NOAA station number, from www.wrcc.dri.edu.

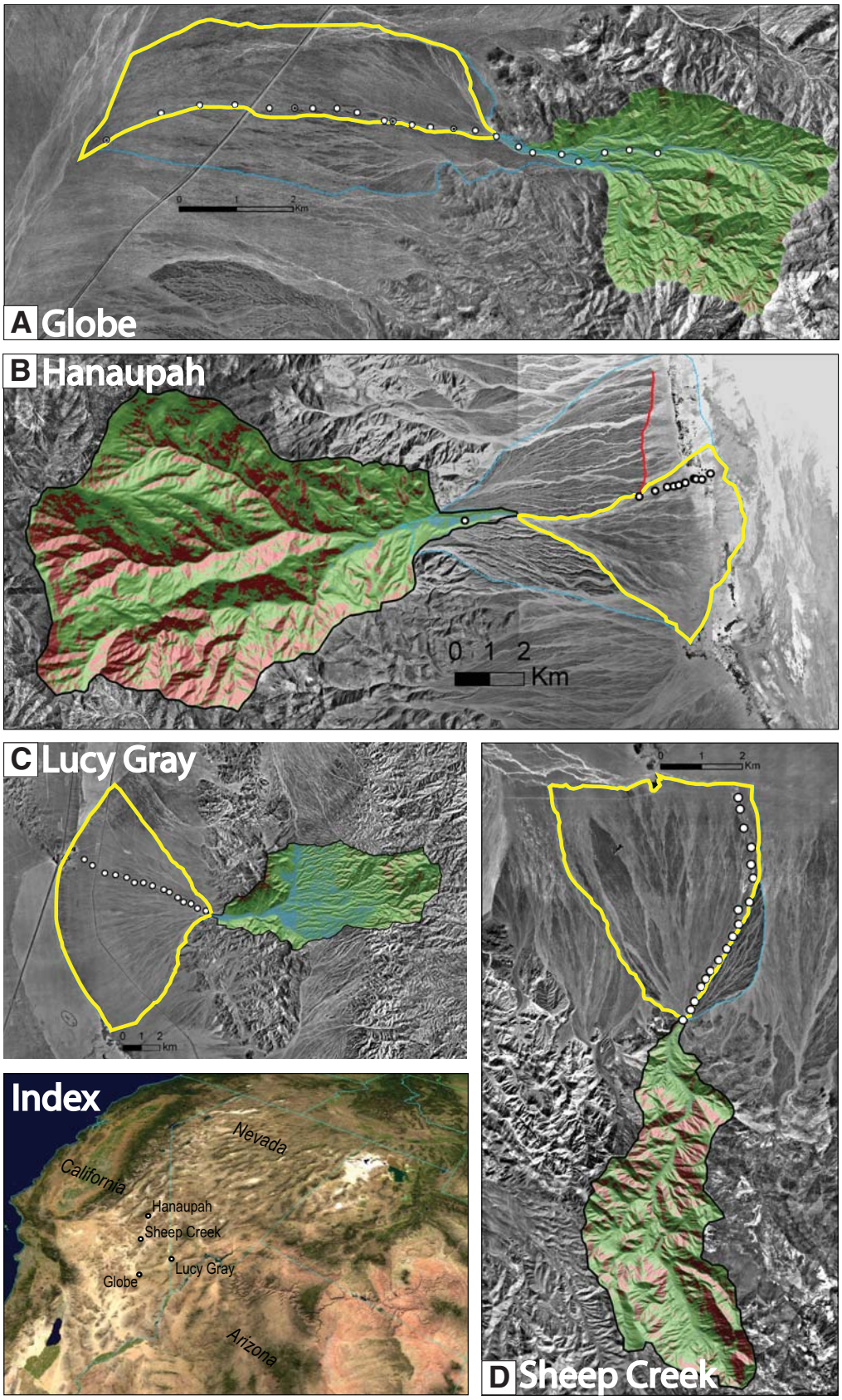

Figure 4. (A) Globe fan in the Providence Mountains, California; (B) Hanaupah fan, Death Valley, California; (C) Lucy Gray fan, California and Nevada; and (D) Sheep Creek fan in the Avawatz Mountains, California. Digital orthophotographs of alluvial fans with source catchments shown as hillshaded 1-m (Globe) or 10-m DEMs, on which are draped 2-m (Globe) or 20-m slope estimates. North is to the top of the images. Blue cells are slopes below 0.10, where channel processes may predominate; green cells are slopes between 0.10 and 0.65, where creep and overland flow transport processes may predominate; and red cells are slopes above 0.65 (~35°), an approximation for the angle of repose. Solid blue lines approximate the lateral boundaries of active sediment transport on the fans; dashed blue lines approximate former boundaries of the fans. Channel cross sections are shown by white dots, starting with 1 at distal end and increasing sequentially upfan. Variations in image albedo on fans represents, in part, differential development of desert varnish on deposits that are largely Pleistocene or older. Note active fault on Hanaupah fan truncating older surface. Source catchments with active faults mapped at their boundaries (Hanaupah and Sheep Creek) tend to have larger source catchment areas above angle-of-repose slopes.

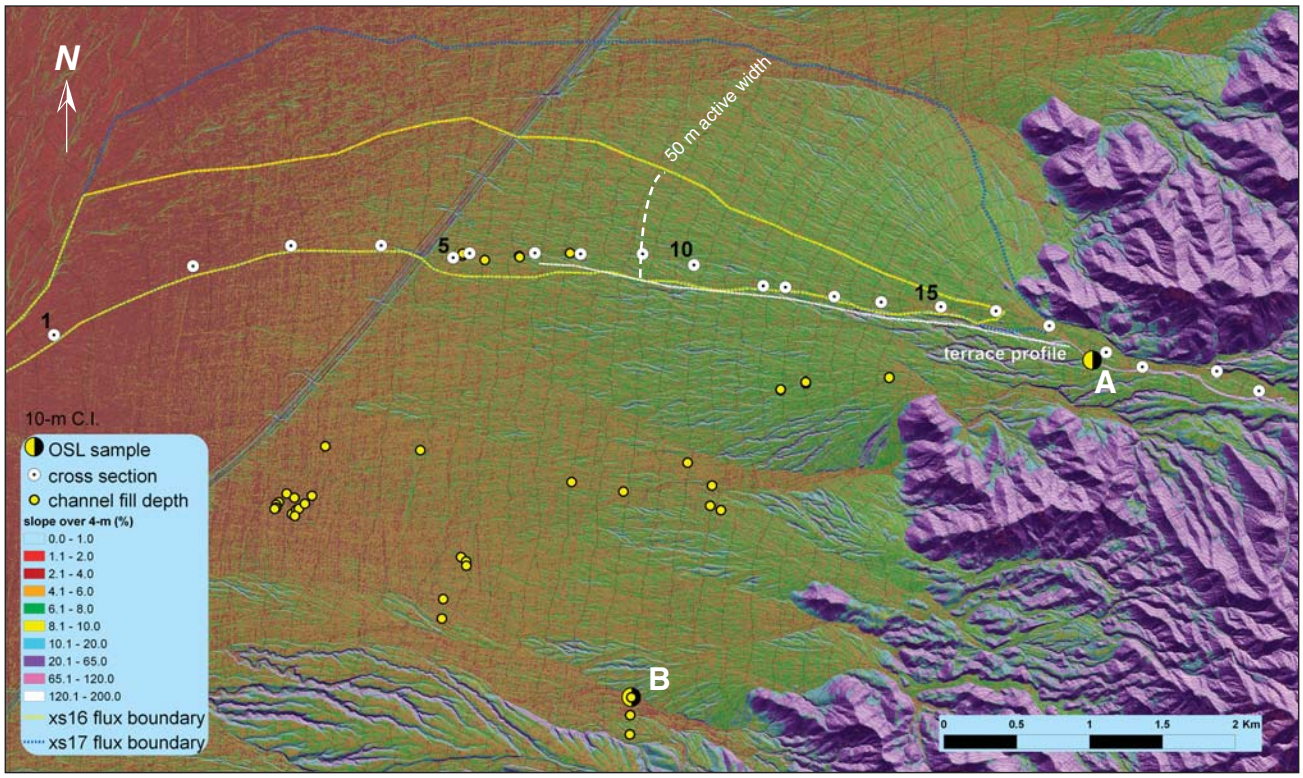

Figure 5. Maximum-fall slope over 4 m, superimposed on 1-m hillshaded LiDAR topography of Globe fan. Channel slopes decline from 0.07 at fan head (greens) to 0.01–0.02 (reds) at junction with axial wash. Cross-section number in Table 3 is shown above white dots representing field cross-section locations. Dashed white line shows crest of older terraces adjacent to modern wash (see Fig. 23). Note fan disruption by railroad and linear artifacts from LiDAR swath lines (~0.3 m in relief). Dashed arc through cross section 9 shows path along which we measured ~50 m of active channel widths, ~10 m more width than present at cross section 16 (see Table 3).

Fan deposits to the south of Globe have been extensively studied by McDonald (1994) and by McDonald et al. (2003), who mapped eight alluvial units whose deposition they argued to be a function of regional climatic transitions. Alluvial fan deposits of Globe and nearby piedmonts are the focus of numerous current interdisciplinary studies, including geoecology (Phelps et al., 2005; Bedford et al., 2007; Miller et al., 2007) and vadose zone hydrology (Miller et al., 2002; Miller et al., 2004; Schmidt et al., 2004; Perkins et al., 2005; Nimmo et al., 2005). Figure 7 illustrates surficial mapping on the southern side of the fan (Miller, 2006, unpublished mapping), where deposits are mapped into four broad categories on the basis of inset relations and pedogenesis as described in the previous section. Historically active deposits (blue) are inset into older deposits that extend to the distal fan as narrow ribs, indicating long-term persistence of fan geometry. Soil pits in active channels on the southern side of the fan revealed indurated, reddened soils with Bw to Bt horizons, at depths less than one meter. Studies of channel hydraulic geometry and scour depth are underway in this area (yellow circles, Fig. 5), and these studies allow crude estimates of the depth of sediment storage in fan channels.

We sampled fine sediment at two sites in the Globe area for luminescence dating to constrain deposition age—a 5.0-m–high fluvial fill terrace (A, Fig. 5) whose age represents the last time of substantial aggradation at Globe fan head and one of the widest channels to the south (B, Fig. 5), to estimate the age of the oldest deposits on the Pleistocene soils. At the fill terrace, we sampled a fine-grained pocket of eolian sediment ~2 m above the active channel. We took adjacent bulk samples from 0.1- to 0.2-m–thick imbricated gravel beds with sand matrix. At a 20-m wide channel south of Globe fan, we excavated a 0.95-m–deep trench to an underlying oxidized, iron-rich soil (Btk) that is likely Pleistocene. Overlying sediments are thin- to medium-bedded (1- to 10-cm) sands locally stratified and cross bedded, with sparse imbricated gravel lenses.

Lucy Gray

The Lucy Gray Mountains and the McCullough Range expose gneissic Early Proterozoic granitoids, associated pegmatitic dike rocks, and Tertiary mafic volcanic rocks whose detritus comprise the Lucy Gray fan. The two ranges are separated by a low-relief belt of early Pleistocene and older alluvium, where Hewett (1956) proposed the pre-Quaternary McCullough fault, with ~6 km of normal displacement, east side up. Snow is not uncommon in the higher elevations of the McCullough Range. Drainage from the McCullough Range transports sediment through a bedrock canyon cut in the Lucy Gray Range, westward toward Ivanpah Valley, where it is deposited in the Lucy Gray fan and the connected Roach and Ivanpah playas (~800 m). Channel proximal surfaces in the Lucy Gray fan have been mapped as Holocene to late Pleistocene (Schmidt and McMackin, 2006), and varnished (low albedo in Fig. 4), undissected deposits over most of the fan indicate minor Holocene subsidence. The fan lacks evidence for Holocene

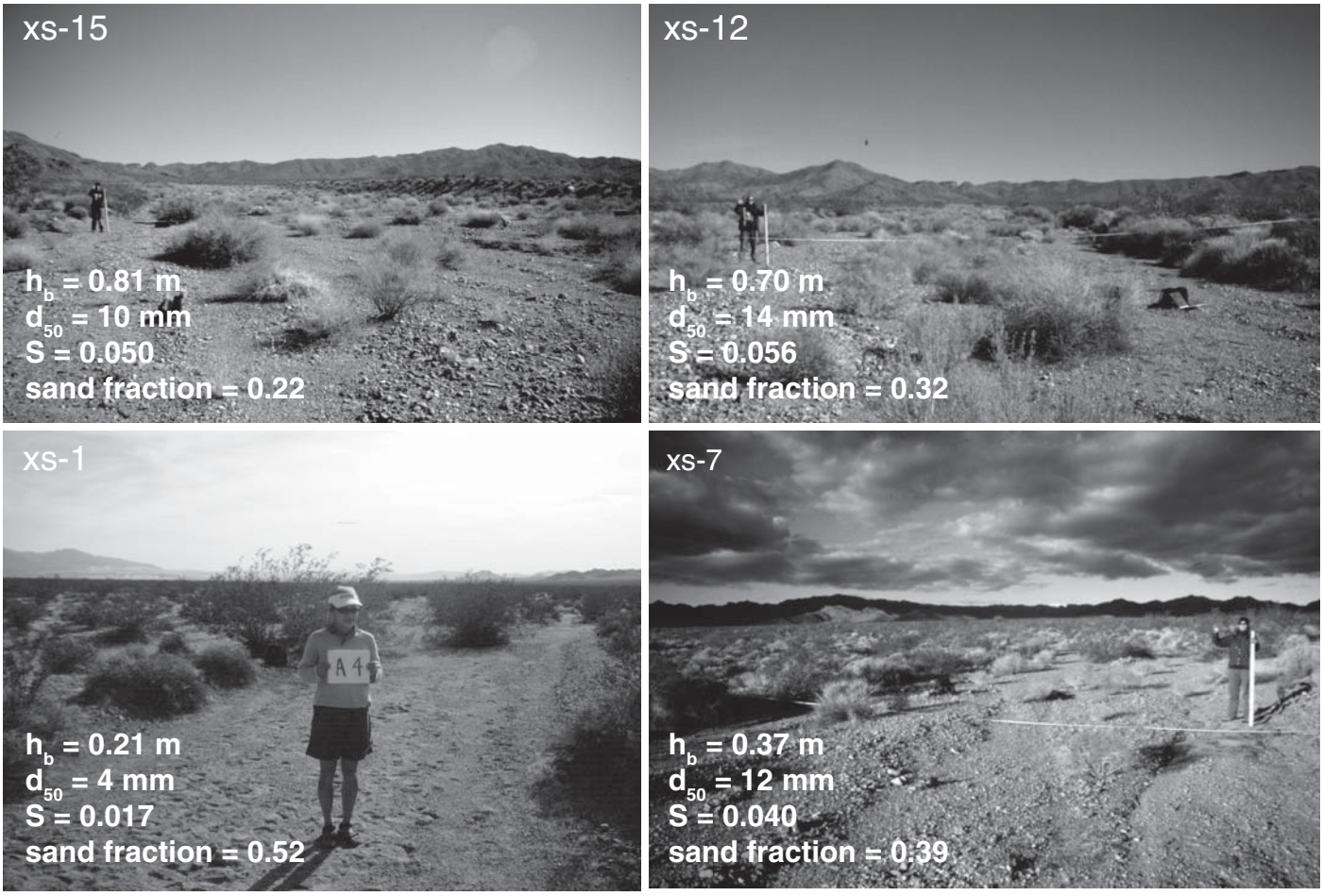

Figure 6. Images of locations on Globe fan, illustrating decline in bankfull depth h_b downfan. Note that while slopes declines in the first three panels from ~0.06 m to ~0.04 m, median gravel size d_{50} does not change significantly. However, sand fraction increases monotonically downfan, consistent with progressive off-channel deposition of gravel.

or late Pleistocene faulting, although a short remnant fault scarp in Pleistocene deposits lies south of the fan (K. House, 2006, oral commun.). The playa provides a local source for eolian sand that is mixed with alluvium in the distal reaches of the fan (Schmidt and McMackin, 2006).

Sheep Creek

The left-lateral Garlock fault terminates at the Avawatz Mountains, a high-relief (e.g., >1000-m) range north of Baker, California. Paleozoic and Proterozoic carbonate and siliciclastic deposits and Mesozoic granitic and metavolcanic rocks (Brady, 1986; Spencer, 1990) are source rocks for alluvial fans on the northern and eastern range fronts. Reverse faults along these margins place rock onto unconsolidated Pleistocene deposits at fan heads, indicating active rock uplift (e.g., Brady, 1986). On the northern front, Sheep Creek fan (Fig. 4) is bounded by active reverse faults at its fan head, and its distal channels join Amargosa Wash, a sand bedded channel. Mapping by Clayton (1988) shows four older, varnished surfaces at Sheep Creek fan, which lie above the active channel. A clay-rich alteration zone in the catchments headwaters produces unusually fine mudflows (e.g., Schmidt and Menges, 2003) whose fine-grained deposits (sandy/clay mixtures) can be found at the Amargosa River at slopes as low as 0.005. By contrast, coarse-grained debris-flow deposits are not evident in the active channels past the fan head.

Hanaupah

Hanaupah fan sediments are derived from steeplands cut in Proterozoic rock (quartzite, dolomite, and argillite) and Tertiary granites of the Panamint Mountains (Albee et al., 1981), a normal fault-bounded block. This source region produces annual snowmelt runoff that may occasionally reach the upper fan. Above active channels, Denny (1965), Hunt and Mabey (1966), Hooke (1972), Dorn et al. (1987), and Hooke and Dorn (1992) have mapped between two and five older fan deposits that darken with desert varnish with age (Fig. 4). These units are probably young to intermediate in age. Using rock varnish dating, Dorn (1996) proposed that four units above the active wash were deposited during 0.5–9.0 ka, 14–50 ka, 105–170 ka, and 490–800 ka. This technique have been challenged by Wells and McFadden (1987), who questioned its utility and application to units such as these. Recent luminescence work by Sohn et al. (2007) showed that deposits equivalent to the youngest two units discussed above have dates of 3.7–13 ka, and 25 ka and older. As with other fans we studied, Pleistocene deposits extend nearly the length of the fan. However, the down-to-the-east Hanaupah fault (Hunt and Mabey, 1966) truncates heavily varnished deposit surfaces in the distal fan (Fig. 4), indicating Pleistocene subsidence. Leveling by Sylvester (2001) indicates that this fault had no detectable surface

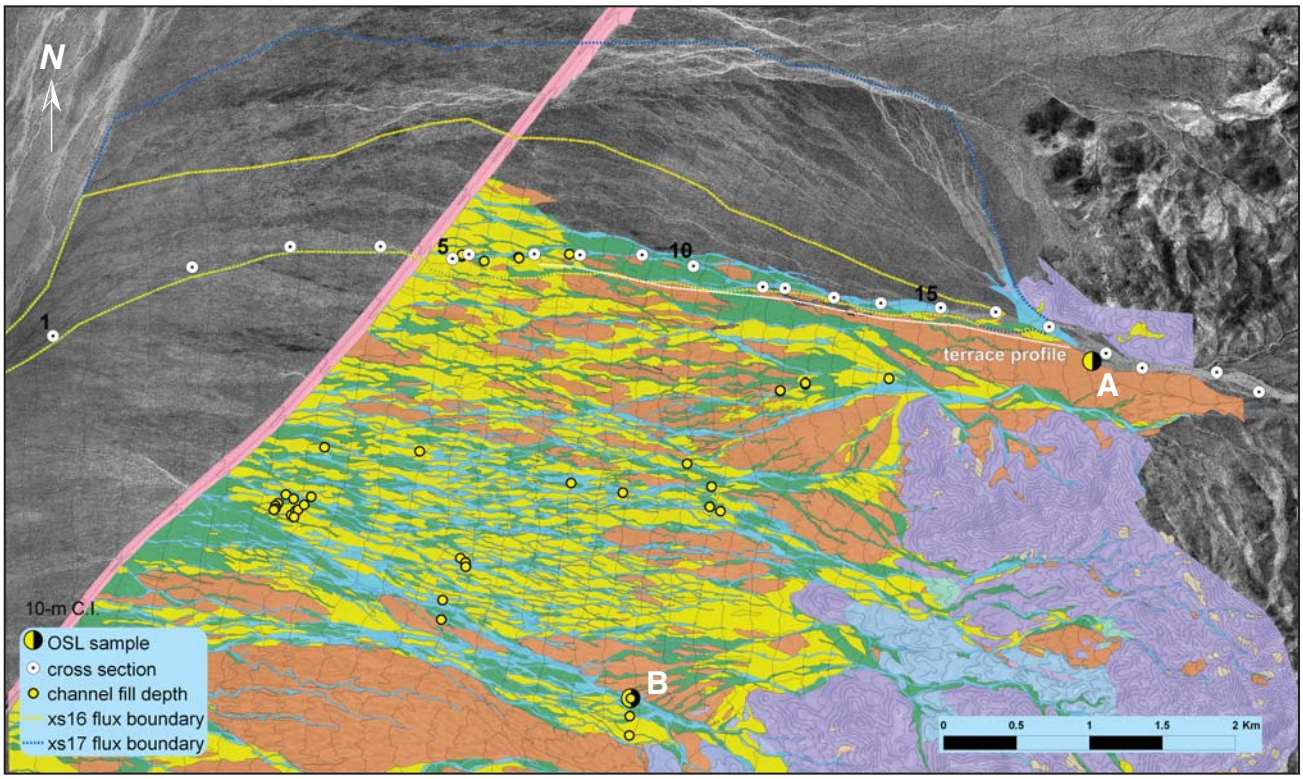

Figure 7. Surficial geologic map of Globe fan and adjacent Hayden piedmont. Bedrock in purple, intermediate-age deposits are shown in yellow, older young deposits in green, and historic active deposits, including active channel bed, in blue. Background is 1-m Digital Orthophoto Quarter Quadrangle (DOQQ). Blue line encloses estimate of Holocene sediment pathways for the entire fan; yellow line encloses area over which sediment passing through cross section 16 is deposited over Holocene.

creep between 1970 and 2000. Lacustrine deposits mark former Lake Manly shorelines in the most distal portion of the fan.

Denny (1965) hypothesized that over an appropriately long timescale, deposition upfan of the Hanaupah fault might be balanced by erosion from older deposits. He measured particle sizes in the active channel by collecting 25 particle diameters at equal spacing along cross sections. He found that geometric mean grain size varied down the active channel between 11 and 24 mm, with no systematic pattern. Work by Ibbeken at al. (1998) used photography to examine planform grain-size distributions at four profiles down the lowest fan surface, which includes active channels. They presented these results as composite distributions and reported no strong downfan trends in grain size. Gravel composition is ~20% granite, 60% quartzite, and 10% carbonate and argillite (Hunt and Mabey, 1966). Hanaupah is widely reported as an example of a debris-flow dominated fan (e.g., Blair and McPherson, 1994b; Ibbeken et al., 1998). Occasional deposits of coarse boulders and matrix-supported lenses in older fill terraces are likely debris-flow deposits. However, both the active channel and most deposits exposed in cut banks are composed of clast-supported, pervasively imbricated gravels with a sandy matrix. Imbrication is consistent with traction transport by water, rather than inertial transport by debris flows.

METHODS

Thread and Sector Selection

To measure hydraulic and grain-size properties downfan, we selected the most active, continuous channel thread traversing the fan center. Center threads have minimal sediment input from fan-marginal sources (e.g., adjacent steeplands or other fans), simplifying the pattern of sediment supply to the channel. We chose the most active thread by finding the widest, least vegetated (high albedo) thread on recent (1980s) U.S. Geological Survey DOQQ (Digital Orthophoto Quarter Quadrangle) coverage. We defined fan head as the point where the single-thread channel first bifurcates downfan (called intersection point by Hooke, 1967, and by Wasson, 1974). Starting just above the fan head, we chose cross sections between every other pair of contours (typically 40 ft) down the main thread to the axial valley or the playa boundary. We mapped the boundaries over which sediment from the highest cross section could be dispersed as a fan sector (e.g., yellow polygon in Fig. 5). Within this sector, we mapped high-albedo, active channels along a contour that includes each measured cross section. Summing these channel widths along each arc provides an estimate of total active channel width, through which the sediment passing the uppermost cross section could be distributed as it travels downfan. Field traverses indicated that these estimates of total widths are within several tens of meters of field-measured values.

Channel Measurements Down-Thread (Bankfull Depth, Width, Reach Slope, Scour Depth, and Bed Texture)

We selected cross-section sites within straight reaches with representative bed texture and abundant self-formed banks. We avoided areas where bank heights were influenced by dense vegetation. We defined bankfull flow top using the highest banks with recent deposition along

a reach, including slackwater fines and gravel lobes that were unvegetated or vegetated with annuals. We defined bankfull depth h_b as the difference between this height and the lowest point along the cross section. We avoided cut banks, which represent past incision rather than the desired estimate of current flow trim lines. To estimate reach slope, we surveyed long-profiles using either handlevel, stadia rod, and tape or laser and tape (Hanaupah). For each long-profile, we surveyed about ten points over a reach length approximately five times the observed bankfull width. The long-profiles were symmetric about the cross section. For channels over ~20 m wide, we used the maximum tape length of 100 m to survey the long-profile. These criteria resulted in point spacing varying from several meters for narrow channels to 10 m for the widest channels. Contour map slopes are 77%–230% of reach slopes (Table 3; Fig. 8), illustrating the need for local measurements. Slopes derived from 1-m LiDAR (light detection and ranging) contour maps closely approximate field values (Fig. 8).

As part of an ongoing study on channel scour depth at Globe fan, we dug trenches between the banks of a second set of randomly selected channels to estimate the depth of recent sediment over older soils (Fig. 5). Recent fluvial sediments are planar beds of sand and gravel that range from 1 to 10 cm thick and lack the red color or fines content of underlying pedogenic layers. The underlying soils are typically brown to red with Bt and Bw horizons and have been dated elsewhere as Pleistocene (e.g., Sowers et al., 1988; Wang et al., 1994; Sohn et al., 2007). Depth to this older horizon is an estimate of long-term maximum scour depth for active channels and approximates the amount of Holocene material stored beneath channel beds. We selected straight reaches to avoid excessive effects of flow convergence or divergence. We sampled channels from ~0.1-m to ~20-m bankfull width to examine variations in long-term scour depth with channel size.

We assumed that during bank forming, likely supercritical flows, sands behave as suspended load. We estimated coarse bed-material (>2-mm) size distributions and bed-surface sand fraction F_{sand} using a random walk technique across the entire channel bed (excluding banks) over an area ~4 m on either side of the cross section. We chose 4 m as an arbitrary value that captures cross-section local conditions but is wide enough that we do not persistently resample the same area. Using a pencil point, we collected intermediate axis measurements for grains >2 mm until we had at least 100 measurements. For narrow or sandy channels, this resulted in covering the area multiple times. For very wide, gravelly channels, this represents one or more traverses; we completed a traverse even after 100 measurements to avoid biasing sampling to a particular channel area. We found that we needed at least 75 counts to reach stable median values in the most poorly sorted channels that we sampled (Fig. 9). We calculated bed sand fraction as the number of <2-mm counts divided by the total number of counts. We calculated bed-material, grain-size distributions excluding sand or finer fractions, unlike most previous studies that lumped all grain sizes together to calculate nonparametric measures (e.g., d_{50}).

LiDAR Topography

We contracted with Airborne 1 to acquire LiDAR topography at Globe with 1-m or denser average point spacing, with the intention of defining channel dimensions and slopes as accurately as possible. We filtered the last return-point data set using TerraSolid Software's TerraScan® program to approximate a bare-earth topographic surface. We kriged these points using Golden Software's Surfer® with linear averaging over a 10-m window, yielding a 1-m grid approximating bare-earth topography. Visual inspection and field checking indicate that the resulting DEM (digital elevation model) contains many local linear artifacts (scale errors?) from laser swath lines with systematically different elevations (e.g., Fig. 5).

Luminescence Dating

We sampled the base of the widest active channel in the field area (B, Fig. 5), and a pocket of fine-grained (eolian?) sediment near the base of the deepest bank exposure (A, Fig. 5) at the fan head. We sampled these deposits at night, driving a PVC (polyvinyl chloride) tube into sample areas and capping the ends of the tube. Shannon Mahan (U.S. Geological Survey, Luminescence Dating Laboratory, Denver, Colorado) processed samples in her laboratory. She discarded end material (~3 cm) from each tube and prepared samples using standard procedures with appropriate modifications (Millard and Maat, 1994; Roberts and Wintle, 2001; Singhvi et al., 2001). Blue-light OSL (optically stimulated luminescence) was done on fine sand-size (125- to 105-micron size) samples, and IRSL (infrared stimulated luminescence) was done on the fine silt-fraction (4- to 11-μm) samples. All sand-size samples were analyzed by single-aliquot regeneration procedures (SAR) (Murray and Wintle, 2000; Banerjee et al., 2001) with blue-light excitation. Dose recovery and preheat plateau tests were performed to ensure that the sediments were responsive to optical techniques and that the proper temperatures were used in producing the D_e values. The fine-grained (4–11 μm) extracts from all samples were dated using the total bleach, multiple-aliquot additive-dose (MAAD) method (Singhvi et al., 1982; Lang, 1994; Richardson et al., 1997; Forman and Pierson, 2002).

MODEL FORMULATION

Threshold and Transport Equations for Steep Alluvial Fans

Shields' criterion predicts that at the threshold of motion for a uniform grain size D,

$$\tau_c = \tau_c^*\left(\rho_s - \rho_w\right)gD \qquad (1),$$

where ρ_s and ρ_w are sediment particle and water density, g is the gravitational constant, τ_c is critical fluid shear stress for initial motion, and τ_c^* is a dimensionless number characterizing resistance to motion (Fig. 3). Approximations of shear stress using the product of hydraulic radius R and slope S ($\rho_w gRS$) are known to be locally inaccurate, but may capture reach-scale variations in shear stress. Using this approximation, (1) can be recast in terms of a threshold slope at bed-material entrainment:

$$S = \tau_c^*\left[\frac{\rho_s - \rho_w}{\rho_w}\right]\frac{D}{R} \qquad (2),$$

assuming form drag is insubstantial. Addition of sine correction terms for steep slopes has a negligible effect on values (third decimal place or lower). If fan slope is set by threshold conditions, and D is represented by the median grain size d_{50}, a plot of d_{50}/R against S should be nonrandom for a constant τ_c^*. We collect these data from the cross sections shown in Figures 4 and 5 and plot it to test this hypothesis.

To test the transport hypothesis, we input hydraulic and grain-size data from the cross sections below fan heads to a bedload transport model and estimate unit bedload fluxes downfan. We use a gravel transport equation that Wilcock and Kenworthy (2002) modified after a surface-based transport model proposed by Parker (1990). The expression was calibrated using measured bedload flux (e.g., Fig. 10) under a variety of flow conditions:

$$W_g^* = \frac{\left(\frac{\rho_s}{\rho_w} - 1\right)gq_{bg}}{F_{sand}\left(\frac{\tau_b}{\rho_w}\right)} = A\left[1 - \frac{x}{\left(\tau_b / \tau_{rg}\right)^{0.25}}\right]^{4.5} \qquad (3),$$

TABLE 3. CROSS-SECTION HYDRAULIC AND GRAIN SIZE DATA

Location	Sample	Total active width (m)	x Downfan (m)	w/d	Slope (50-m)	Slope (7.5')	w_b (m)	h_b (m)	R (m)	Sand fraction	d_{50} (mm)	d_{16}	d_{25}	d_{75}	d_{84}	Mode[2] (mm)	IQR[†] (mm)	σ[#] (mm)	h_b/d_{50}	τ*
Globe	Kelso wash	–	7469	1630	0.015	0.015	750	0.46	0.46	–	–	–	–	–	–	–	–	–	–	–
	1	*50*	7290	30	0.017	0.020	6.2	0.21	0.14	0.52	4	2	2	7	10	4	5	0.45	53	0.36
	2	50	6294	20	0.024	0.022	5.3	0.27	0.14	0.44	5	3	3	9	15	6	6	0.45	54	0.41
	3	50	5502	34	0.034	0.033	9.1	0.27	0.18	0.41	6	3	4	15	22	7	11	0.37	45	0.63
	4	80	4860	46	0.036	0.043	12.9	0.28	0.17	0.42	4	2	3	7	12	5	4	0.41	70	0.92
	5	60	4284	19	0.040	0.054	6.4	0.33	0.22	0.47	13	5	6	25	34	13	19	0.38	25	0.41
	6	70	4098	80	0.042	0.054	31.2	0.39	0.23	0.44	15	4	6	27	45	14	21	0.30	27	0.40
	7	50	3708	43	0.040	0.052	16	0.37	0.25	0.39	12	5	6	23	34	13	17	0.38	32	0.53
	8	65	3342	35	0.048	0.038	11.9	0.34	0.16	0.39	10	4	5	26	37	11	21	0.33	34	0.47
	9	70	2904	65	0.046	0.062	24	0.37	0.21	0.34	11	5	6	24	34	12	18	0.38	34	0.53
	10	80	2544	46	0.053	0.057	23.5	0.51	0.35	0.27	13	5	6	23	31	12	17	0.40	41	0.91
	11	70	2010	72	0.058	0.069	50.2	0.70	0.42	0.33	16	6	7	33	46	16	26	0.36	45	0.96
	12	70	1866	82	0.056	0.052	57.2	0.70	0.29	0.32	14	6	7	33	49	16	26	0.35	50	0.71
	13	50	1500	56	0.050	0.056	26.2	0.47	0.32	0.33	12	5	7	22	31	12	15	0.40	41	0.85
	14	80	1158	58	0.055	0.052	37.5	0.65	0.41	0.22	10	5	6	21	29	11	15	0.42	65	1.36
	15	60	786	59	0.050	0.060	47.6	0.81	0.45	0.22	10	4	6	16	23	10	10	0.42	81	1.38
	16	100	402	–	0.057	0.069	54.1	–	–	0.22	11	5	7	25	36	13	18	0.37	–	–
	17	100	0	65	0.047	0.060	96.6	1.49	0.85	0.34	14	4	6	35	46	14	29	0.29	110	1.79
	18	–	-378	71	0.054	0.057	56	0.79	0.35	0.32	23	7	11	42	56	21	31	0.35	35	0.51
	19	–	-738	–	0.051	0.051	69.4	–	–	0.28	17	5	6	36	50	16	30	0.32	–	–
	20	–	-1134	78	0.053	0.049	48.6	0.62	0.37	0.33	18	4	7	30	44	15	23	0.30	34	0.66
	21	–	-1524	84	0.050	0.054	80.9	0.96	0.46	0.31	20	7	9	40	49	19	31	0.38	48	0.70
	22	–	-2256	60	0.063	0.067	38.3	0.64	0.28	0.23	15	5	6	32	42	14	26	0.35	44	0.72
	23	–	-2580	72	0.058	0.056	44.6	0.62	0.34	0.23	25	7	9	44	51	21	35	0.37	25	0.48
	24	–	-3066	57	0.062	0.060	44.8	0.79	0.37	0.18	14	5	7	28	36	14	21	0.37	56	0.98
Sheep Creek	Amargosa	–	5286	1027	0.006	0.01	380	0.37	0.37	–	–	–	–	–	–	–	–	–	–	–
	1	49	5286	27	0.014	0.013	7	0.26	0.15	0.70	9	3	4	20	55	11	16	0.23	29	0.14
	2	28	5010	18	0.023	0.026	8.05	0.44	0.24	0.61	10	3	4	24	38	10	20	0.28	44	0.34
	3	28	4770	33	0.031	0.031	9.1	0.28	0.18	0.59	19	4	6	49	79	18	43	0.23	15	0.18
	4	42	4380	37	0.04	0.043	20.8	0.56	0.30	0.44	25	3	5	64	94	19	59	0.18	22	0.29
	5	35	4014	28	0.043	0.038	19.5	0.70	0.43	0.42	24	4	6	54	67	19	48	0.24	29	0.46
	6	49	3612	21	0.046	0.049	16.5	0.78	0.43	0.34	33	8	13	54	65	26	41	0.35	24	0.37
	7	20	3096	11	0.05	0.062	9.4	0.88	0.56	0.28	30	8	11	52	62	25	41	0.36	29	0.56
	8	35	2982	16	0.052	0.062	14.2	0.87	0.46	0.24	40	8	19	70	85	30	51	0.31	22	0.37
	9	28	2574	41	0.052	0.051	23.2	0.57	0.38	0.26	35	6	12	63	88	26	51	0.26	16	0.34
	10	49	2280	19	0.055	0.051	17.7	0.91	0.44	0.28	61	8	21	94	111	38	73	0.27	15	0.24
	11	35	1962	30	0.059	0.071	24.3	0.80	0.43	0.24	35	11	16	61	76	31	45	0.38	23	0.44
	12	35	1650	21	0.056	0.129	14.4	0.69	0.42	0.17	20	6	8	42	55	19	34	0.33	35	0.71
	13	20	1404	27	0.065	0.071	26.1	0.96	0.54	0.30	33	5	10	52	67	22	42	0.27	29	0.65
	14	20	1062	14	0.073	0.068	13.6	0.98	0.50	0.30	19	5	9	41	49	17	32	0.32	52	1.17
	15	49	822	31	0.071	0.068	21	0.67	0.31	0.21	28	5	8	53	70	21	45	0.27	24	0.47
	16	21	534	20	0.068	0.079	18.8	0.96	0.70	0.15	21	6	11	41	48	18	30	0.35	46	1.37
	17	56	288	40	0.069	0.084	29.9	0.75	0.43	0.26	27	6	11	41	46	20	30	0.36	28	0.66
	18	35	0	21	0.071	0.068	25.6	1.23	0.54	0.22	27	9	14	48	56	24	34	0.40	46	0.86

(continued)

TABLE 3. CROSS-SECTION HYDRAULIC AND GRAIN SIZE DATA *(continued)*

Location	Sample	Total active width (m)	x Downfan (m)	w/d	Slope (50-m)	Slope (7.5')	w_b (m)	h_b (m)	R (m)	Sand fraction	d_{50} (mm)	d_{16}	d_{25}	d_{75}	d_{84}	Mode (mm)	IQR† (mm)	σ# (mm)	h_b/d_{50}	τ*
Hanaupah	1	*50*	4990	16	0.005	0.005	2.3	0.14	0.14	1.00	1	1		1	1	1	0	1.00	140	0.42
	2	*50*	4689	22	0.012	0.006	7.35	0.33	0.16	0.47	6	3	4	9	10	6	5	0.54	55	0.19
	3	*50*	4584	36	0.019	0.020	7.6	0.21	0.10	0.43	13	5	5	27	35	13	22	0.37	16	0.09
	4	*50*	4500	16	0.021	0.020	7.2	0.46	0.11	0.30	27	6	8	43	60	21	35	0.32	17	0.05
	5	56	4015	14	0.046	0.041	8	0.58	0.33	0.28	30	7	15	66	90	27	51	0.28	19	0.31
	6	84	3819	14	0.045	0.049	12.1	0.84	0.46	0.30	49	5	14	102	141	33	88	0.19	17	0.26
	7	63	3672	11	0.055	0.059	10.5	0.97	0.50	0.26	26	6	8	73	112	26	65	0.23	37	0.64
	8	77	3500	17	0.058	0.067	16	0.94	0.66	0.20	23	7	10	88	130	28	78	0.23	41	1.01
	9	77	3105	34	0.067	0.074	30.7	0.89	0.53	0.14	24	8	12	80	99	27	68	0.28	37	0.89
	10	49	2636	25	0.059	0.052	29.8	1.19	0.69	0.16	24	7	11	55	81	24	44	0.29	50	1.02
	11	–	-2674	57	0.068	0.074	90.2	1.58	1.04	0.02	30	8	15	54	55	24	39	0.38	53	1.43
Lucy Gray	1	400	7545	47	0.014	0.024	7.1	0.15	0.15	0.80	7	4	4	13	17	8	9	0.49	21	0.18
	2	340	7035	57	0.025	0.029	12	0.21	0.09	0.70	7	3	4	12	16	7	8	0.43	30	0.20
	3	610	6195	44	0.026	0.038	8.8	0.20	0.13	0.62	10	5	6	19	23	11	13	0.46	20	0.21
	4	550	5495	31	0.028	0.036	10.3	0.33	0.10	0.61	15	5	6	31	36	14	25	0.37	22	0.12
	5	420	4840	35	0.029	0.043	8.4	0.24	0.17	0.62	11	6	7	22	26	12	15	0.48	23	0.28
	6	390	4280	24	0.026	0.045	6.3	0.26	0.17	0.50	20	7	9	41	50	19	32	0.37	13	0.13
	7	330	3705	45	0.038	0.053	9.55	0.21	0.16	0.50	22	6	8	52	67	21	44	0.30	10	0.17
	8	180	3225	68	0.034	0.053	13.5	0.20	0.16	0.44	21	7	10	50	61	21	40	0.34	10	0.16
	9	180	2755	17	0.044	0.048	9	0.52	0.30	0.37	14	5	7	29	46	15	22	0.33	39	0.60
	10	140	2260	23	0.041	0.055	10.1	0.44	0.30	0.44	15	7	8	34	43	17	26	0.40	29	0.49
	11	140	1805	43	0.036	0.055	23.6	0.55	0.35	0.42	17	6	8	40	54	18	33	0.33	32	0.45
	12	180	1355	26	0.047	0.061	11.2	0.43	0.33	0.44	23	7	10	46	65	22	36	0.32	19	0.42
	13	80	915	46	0.036	0.053	17.6	0.38	0.37	0.41	16	6	7	44	54	17	37	0.33	25	0.52
	14	70	445	81	0.048	0.049	32.5	0.40	0.46	0.40	24	7	11	61	83	24	50	0.29	17	0.55
	15	130	0	72	0.044	0.069	36.7	0.51	0.42	0.37	23	8	10	48	71	24	38	0.33	22	0.49

†Interquartile Range
#Standard deviation

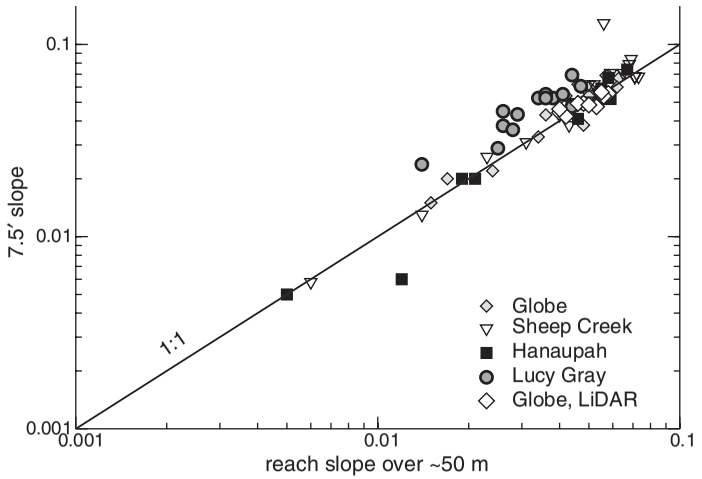

Figure 8. Plot of reach slope against contour-map slope, illustrating requirement for local measurements. Channel slopes from 7.5′ contour maps are 77%–230% of reach-slope values, often higher because field channel lengths tend to be longer (i.e., more sinuous) than estimates from 7.5′ maps. By contrast, LiDAR slopes shown for Globe are 89%–115% of reach values, closer because they are better approximations of the channel length observed in the field.

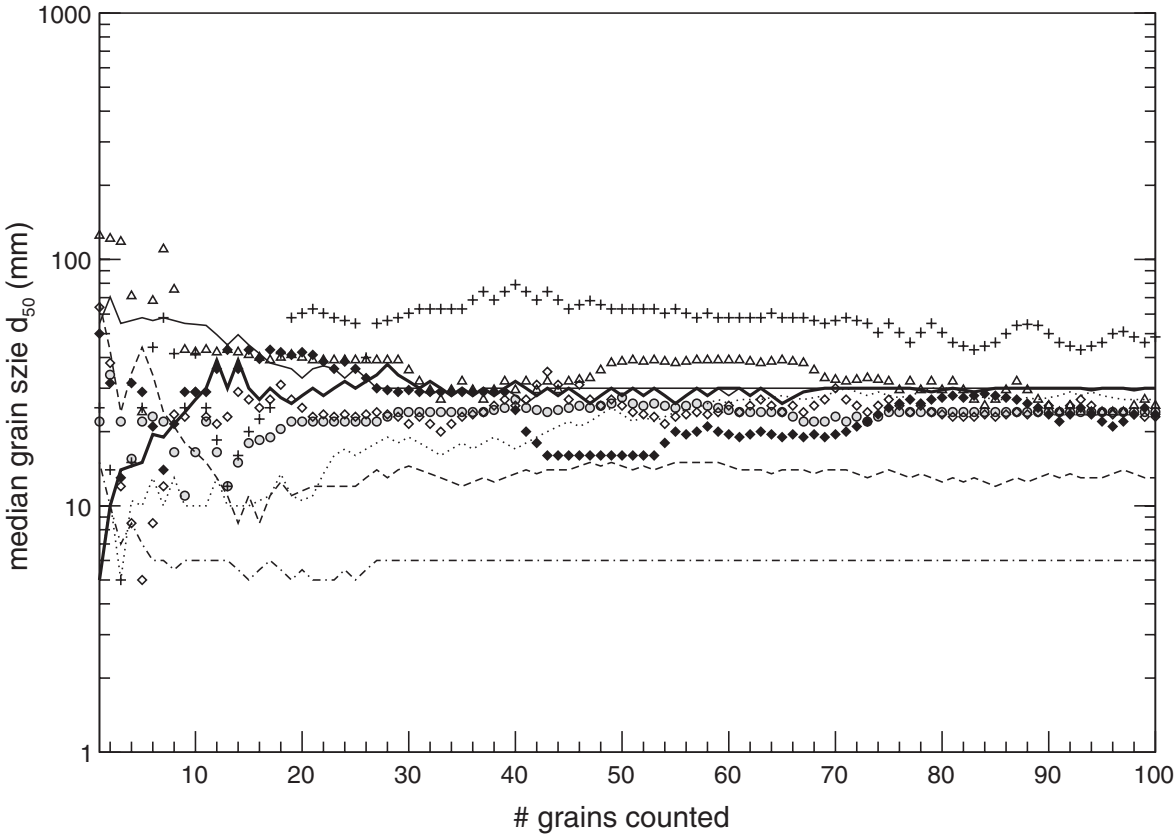

Figure 9. Plot of median value of cross-channel point count as a function of the count number for cross sections of the Hanaupah fan, the most poorly sorted channels of the study sites. Median values tend to stabilize above ~75 counts, indicating that 100 counts are probably a minimum number of gravel counts to reach a stable median value in this environment.

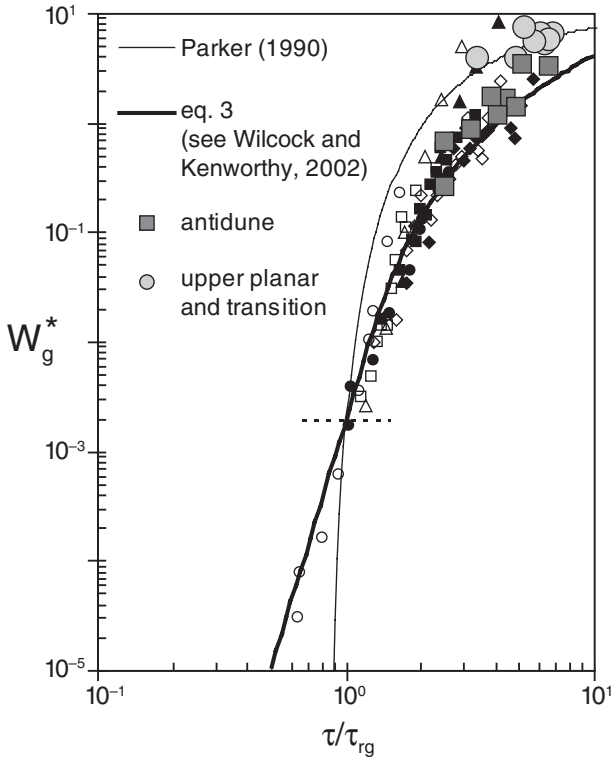

Figure 10. An attempt to validate the use of low-gradient, gravel-transport equations for high-gradient, supercritical flow on fans. Plot of nondimensional shear stress for gravel fraction (τ_b/τ_{rg}) against nondimensional gravel-transport rate W_g^*, after Wilcock and Kenworthy (2002). Small symbols represent gravel-transport rates measured in lower gradient (typically <0.03 slope) gravel-bed rivers and used to calibrate versions of Equation (3). Larger stippled circles and squares are gravel transport rates from supercritical flow in a flume (Ikeda and Iseya, 1988), with τ_{rg} calculated using Wilcock and Kenworthy's (2002) subsurface sand-fraction model (their Equation 8). Thick solid line is Wilcock and Kenworthy's Equation 4 for gravel transport [Equation (3) in this paper], with A = 115. Thin line is the Parker (1990) transport function. We find that an exponent of –6 in Equation (4), rather than the suggested –25, best fits the experimental data to the bold line representing Equation (3), but the difference is not striking. Close fit of supercritical flume data to transport rates observed elsewhere is consistent with the use of Equations (3) and (4) to model gravel transport on steep fan channels with supercritical flow. Note the underprediction of transition and upper planar transport rates, probably as a result of reduced flow resistance.

where W_g^* is nondimensional unit gravel flux q_{bg}, F_{sand} is surface bed sand fraction, and the parameters A (= 115) and x (= 0.923) have values estimated in Wilcock and Kenworthy (2002). The quotient τ_b/τ_{rg} is the nondimensional critical shear stress τ^*_c for gravel entrainment, or τ^*_{rg}.

A further adjustment reduces τ^*_{rg} as surface-bed sand fraction increases, using an expression proposed by Wilcock and Kenworthy (2002):

$$\tau^*_{rg} = \left(\tau^*_{rg}\right)_1 + \frac{\left(\tau^*_{rg}\right)_0 - \left(\tau^*_{rg}\right)_1}{\exp\left[14F_{sand}\right]} \qquad (4),$$

where τ^*_{rg} is the reference nondimensional stress for gravel at the threshold of motion, $(\tau^*_{rg})_1$ is this stress for a bed of 100% gravel, and $(\tau^*_{rg})_0$ is the equivalent stress for a bed with negligible gravel. Following Wilcock and Kenworthy (2002), we set $(\tau^*_{rg})_0 = 0.0350$ and $(\tau^*_{rg})_1 = 0.011$.

We apply Equations (3) and (4) to alluvial fan channels, using the cross-section values of shear stress τ_b and sand fraction F_{sand} (Table 3) and τ^*_g values calculated from (4). At the uppermost fan cross section (e.g., 16 in Fig. 5), we calibrate (3) by finding the unit flux that reproduces the observed channel slope for the measured bed material and hydraulic radius R. At the next downfan cross section, we repeat this procedure, with the additional step of partitioning flux across the total active channel width in the sector. We repeat this procedure downfan to generate a plot of unit bed-material flux versus downfan distance.

This procedure has a number of implicit assumptions, which can be summarized in approximate order of decreasing supporting evidence:

- For purposes of late Holocene timescale sediment budgets, there are negligible amounts of gravel deposited in active channel beds.
- For purposes of transport calculations, there is negligible production of sediment on the fan so that unit bedload flux does not increase below the fan head.
- Coarse particle (gravel) flux controls slope.
- Equation (3) provides an unbiased estimate of bedload flux.
- Spatial variations in form drag downfan are negligible.
- Bankfull flows set transport rates that control reach slope.
- Observed bankfull depths correspond to depth during active transport.
- Mainstem shear stresses are characteristic of smaller threads.
- Gravel flux from fan-head channel can be divided into distributary channels downfan in proportion to channel width.
- Variations in flow intermittency downfan are small enough to have marginal effects on transport rate.

There is evidence that is consistent with some of these assumptions. For instance, older deposits above active washes (Fig. 7) and shallow channel scour depths indicate that subsidence cannot be invoked to store large amounts of gravel, at least over Holocene timescales. We assume that production of sediment on the fan is negligible compared to source catchment, so that unit gravel flux declines monotonically downfan. We know this assumption is locally violated because we have observed small catchments from desert pavement areas on the fan contributing sediment. However, these volumes appear to be subordinate to that produced from an actively eroding source catchment. The assumption that channel slope is adjusted to transport gravel flux rate is consistent with the observation that gravel fractions tend to cover most of the bed (Table 3). We test the assumption that (3) is an unbiased estimate of bed-material transport down ephemeral, steep fan channels in the next section. We evaluate the assumption that spatial variations in form drag do not dominate transport rate downfan by plotting the variation in relative roughness downfan in the Results section. We assume that flow conditions at bankfull set channel slope, a proposition that has been argued in perennial rivers, although it has yet to be shown in arid regions. Experimental studies by Hooke (1967) and Hooke and Rohrer (1979) indicate channel-bed aggradation during transport followed by degradation on the declining hydrograph limb. To the degree this sequence occurs on natural fans, we overestimated flow depths from active bank heights. However, the downfan pattern of reduced bank height implies similar decreases in flow depth, even if we overestimate its magnitude. We also apply mainstem values of shear stress to other active channel threads across the arc. This has the tendency to overestimate fluxes on smaller channels, although the proportion of smaller channels across many arcs tends to be low (Table 3). To distribute sediment down the fan segment, we assume that gravel flux is distributed by proportion to channel width, which we have no way of testing. Nor can we evaluate the role of the frequency of flow and transport events (intermittency) downfan.

Test of Transport Equation Using Flume Data

We can test whether Equation (3) is reasonable to apply to fan channels that are steep ($0.01<S<0.10$) and have ephemeral, likely supercritical flow with high relative roughness ($h_b/d_{50}<100$). These conditions are different from the low slope (<0.02) perennial gravel-bedded rivers with low relative roughness values (e.g., h_b/d_{50} values of 100–1000) on which (3) has been calibrated. Many models of roughness on fan channels suggest critical or supercritical flow (e.g., Dawdy, 1979; Edwards and Thielmann, 1984; French, 1987; Blair and McPherson, 1994a). The sole direct measurements that we are aware of for flow on alluvial fans (Rahn, 1967; Beaumont and Oberlander, 1971) indicate standing waves during a flow event and Froude (Fr) numbers far greater than 0.8. These observations suggest that the major sediment transport flows on most fans with substantial sand likely involve standing waves, antidunes, and chutes-and-pools, at Fr greater than 0.8 (Table 1).

We know of no field data that can be used to evaluate the effect of supercritical flow conditions on conventional bedload transport equations. Therefore, we use data from the nearest flume analog to ask the question whether (3) is defensible to use under steep, supercritical flow. We substitute Ikeda and Iseya (1988) data into (3) and plot predicted, nondimensional shear stress against measured bedload flux rate (larger, stippled symbols in Fig. 10), and against unit bedload flux predicted using the subsurface model of Wilcock and Kenworthy (2002). This subsurface model differs from the surface model (4) in that it uses volumetric sand fraction, the parameter reported by Ikeda and Iseya (1988) and a slightly different fit for the influence of sand on τ^*_{rg} (Equation 8 with subsurface parameters from Wilcock and Kenworthy, 2002, Table 3). We calculate τ_b from the depth-slope product of flume flow and correct for side-wall drag using the formula from Williams (1970). Plots of the Ikeda and Iseya (1988) data in Figure 10 are well approximated by Equation (3) predictions, which are shown as a bold line. This is consistent with the use of (3) to model gravel transport on steep alluvial fan channels where bankfull flow is probably also supercritical.

RESULTS

Table 3 lists field data from the channels of alluvial fans in Table 2. To our knowledge, data in Table 3 represent the most complete data set yet collected for alluvial fan channels dominated by traction transport. For this reason, we illustrate patterns of hydraulic and texture data from the subset of the data in Figures 11–9.

Hydraulic Geometry

Figure 5 illustrates the downfan decrease in channel slope along the Globe fan using 1-m LiDAR topography. Slopes are close to field-surveyed reach slopes (Fig. 8); therefore, this

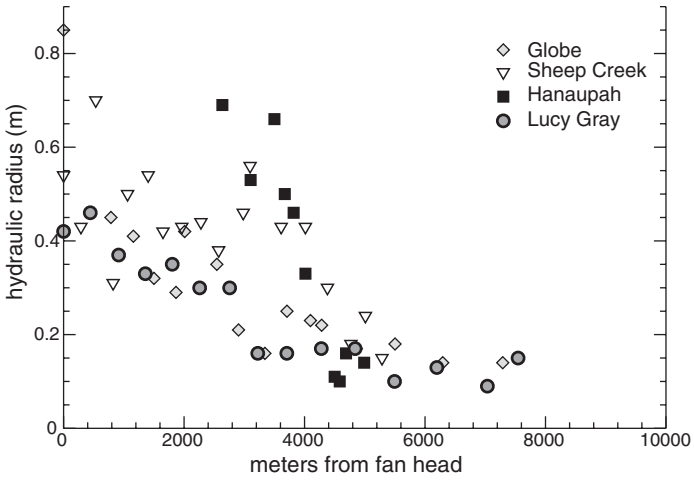

Figure 11. Downfan decline in hydraulic radius.

Figure 12. Gravel bar near cross section 8 on Globe fan, illustrating movement of bed material overbank.

LiDAR topography does approximate field measures of channel slope. Although field-surveyed slopes may be locally different from those measured from U.S. Geological Survey 7.5′ topographic maps (e.g., Fig. 8), the pattern of downfan slope decline from ~0.10 at fan heads to slopes approaching 0.01 at distal channels is not substantially different.

Figure 11 illustrates a downfan decline in hydraulic radius, from values of 0.5–0.9 m at fan heads, to values of 0.1–0.2 m at distal fan channels. These values lie within the range reported by other authors (e.g., Wasson, 1977; Field, 2001). Downfan from these channels, banks are poorly expressed or not present. For all fans, there is a rapid, often exponential decline in hydraulic radius. For fans with no recent faults (Globe and Lucy Gray), the exponential decline is followed by a linear reduction in hydraulic radius at a rate of ~10^{-5} m/m in the lower part of fan.

Locally, banks have been overridden by pulses of bed material that are present as narrow tongues of gravel just overbank (Fig. 12). These deposits are commonly found overbank near channel bends, where the inertia of bed material appears to have carried it up and over the channel bank into older Active or Young alluvial terraces. Similar deposits can be found as wake-zone effects downstream from large bushes, boulders, or other channel obstructions.

Width-to-depth ratios for most fan channels are between 10 and 100 (Table 3; Fig. 13). Many fans have channels with approximately constant width-to-depth ratios (parallel lines in Fig. 13). As bankfull depths grow shallower downfan, they grow proportionally narrower. Exceptionally, channels of the Globe and Lucy Gray have more variable width-to-depth ratios, with those of Globe fan narrowing more rapidly downfan than they shallow.

Scour Depth

Figure 14 illustrates recent sediment deposits that increase in depth from centimeters to ~100 cm as channel bankfull width increases from ~0.1 m to 20 m. Episodic burial and channel scour into the underlying, moderately indurated soils postdates Pleistocene to earliest Holocene-aged soils at these sites (Fig. 5). Luminescence dates from the base of one 20-m–wide channel (B in Fig. 5) range from 5.5 ka (OSL) for the sand fraction to 12.7–15.5 ka (IRSL) for the fine silt fraction (Table 4). The fine-silt mode with the older IRSL age is distinct from the rest of the sample. The finer material is plausibly a separate, partially bleached population deposited from a turbid water column into the pores of a fully bleached sand layer. The dates indicate late Pleistocene to Holocene deposition in the channel, with the most likely time of peak scour at ca. 5 ka. Together with Figure 14, relative and absolute age dating indicates that large amounts of sediment cannot be stored in Globe channel beds over late-Pleistocene to Holocene timescales.

By contrast, sample A from the fan-head fill terrace is at least 72 ka, and possibly older, as it is either saturated or close to saturation for luminescence (see dose rates in Table 4). This minimum date indicates that deposition (and probably sediment-supply rate) at the Globe fan head has been lower for many multiples of Holocene time. It also indicates that the last incident of bedrock-channel incision at this location must be substantially older than 72 ka because of the heavily indurated fanglomerate in the channel thalweg nearby.

Granulometry

Figure 15 shows the lack of gravel fining over the upper 60%–80% of fan-channel length. Sheep Creek fan has the coarsest median values of ~30 mm, roughly three times larger than those observed at similar downfan distances with the Globe fan. Other percentiles (Table 3) have similar patterns, showing no detectable fining in the upper half or more of the fan. All fans show fining after ~4 km downfan, distances where bankfull depth on all four fans converge to values of ~1/3 m, and reaches have 50%–60% gravel, as well as sandy patches. Figure 16 illustrates a decline in bed-area gravel fraction, from values of 0.6–0.9 at fan heads, to values below 0.5 at lower fan boundaries. The pattern is consistent with field observations of overbank lobes of coarse gravel (Fig. 12), indicating off-channel deposition of part of the coarse bed material over older Active or Young alluvial deposits. On Globe fan, patches of fines begin to appear in the channel at gravel fractions below 60%–70%, corresponding to slopes <0.05. Figure 15 indicates that (1) substantial gravel deposition occurs downfan, and (2) τ^*_c can be expected to decline downfan as bed sand fraction increases (e.g., Wilcock and McArdell, 1993). This reduction would tend to increase bedload flux in the absence of other changes.

Test of Threshold

We test the threshold explanation for fan-channel slope (2) by plotting reach slope against the ratio of median grain size to hydraulic radius, assuming constant τ^*_c. If the reduction in median grain size is the primary control on reach slope, we expect a nonrandom, positive

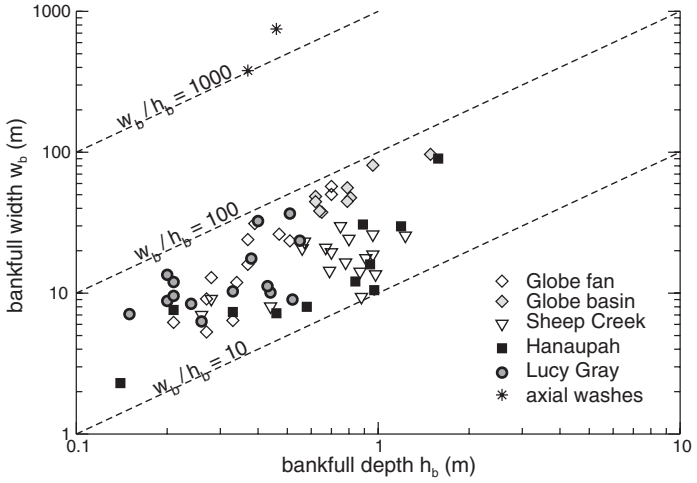

Figure 13. Plot of bankfull depth versus width for fan channels. Lines show constant values of width-to-depth ratios. With the exception of Lucy Gray and Globe, the channels on fans tend toward a constant ratio between 10 and 100.

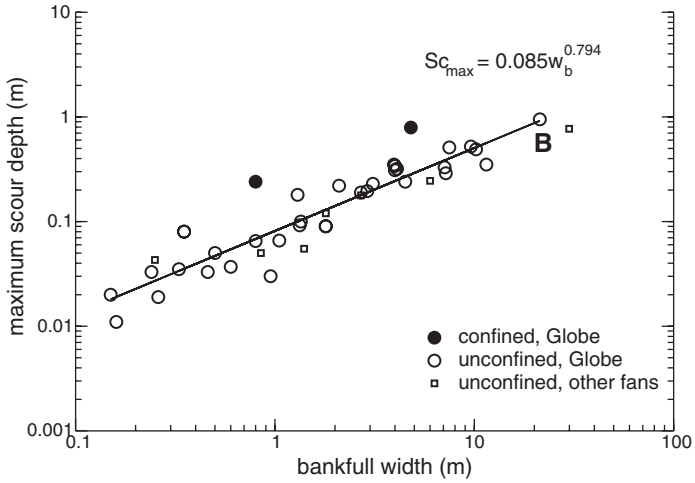

Figure 14. Plot of recent deposit depth over Pleistocene soils against bankfull width for channels of Globe fan. Optically stimulated luminescence (OSL) date at the base of the widest channel (B) is ca. 5 ka, consistent with Holocene age for channel fills.

correlation between local slope and the ratio of grain size to hydraulic radius. A plot of these variables from the four fan mainstem channels in Figure 17 indicates that there is no strong correlation of reach slope with the ratio of grain size to hydraulic radius. The data are inconsistent with a threshold entrainment explanation for fan-channel slope.

Test of Transport

To illustrate downfan patterns in resistance to transport, and transport capacity, we plot relative roughness (Fig. 18) and τ^* (Fig. 19) down the main axial channels of the four fans. There is no strong pattern in relative roughness. However, transport capacity declines exponentially down all fans as hydraulic radius decreases, while median gravel size remains approximately constant in upper and middle reaches. These relations indicate that in the absence of other effects, decreases in hydraulic radius substantially reduce transport rates downfan. Only if τ^*_c reductions with increasing sand fraction are large, or channels bifurcate very rapidly so that the load in any one channel is greatly reduced, can total bedload fluxes be relatively constant downfan.

We explore the effects of channel bifurcation and τ^*_c reductions on transport at Globe fan by using (3) to predict changes in channel slope down Globe fan, assuming no gravel deposition downfan as the null hypothesis. We calculate this flux as the value in (3) that reproduces the observed reach slope at the fan-head cross section. As Figure 20 indicates, even with declining τ^*_c and modest increases in total channel widths, this exercise predicts that fan-channel slope must increase downfan as R declines, even with compensating effects of reductions in τ^*_c and spreading of flux into distributary channels. These results indicate that any transport explanation for these fan slopes must incorporate a term for reduction in gravel flux downfan, as hypothesized by Drew (1873).

Following the method outlined above, we ask what values of unit bedload flux are required to match observed reach slope at each of the fan sites. The resulting graph (Fig. 21) illustrates the pattern of the reduction in bedload flux required, if there are: (i) no errors in field data; (ii) the transport Equation (3) is appropriate; (iii) the τ^*_c correction is appropriate; and (iv) smaller channels along the contour arc hydraulic radii equivalent to the mainstem. The pattern is dominated by an exponential decline in required unit gravel flux downfan. The length over which half of the load is lost varies from ~800 m to 1400 m for fans with no intersecting faults, and is much shorter for the Hanaupah fan (200 m) with a mid-fan normal fault, and a nearby lacustrine lower boundary. These loss rates are likely minimums because condition (iv) overestimates the transport capacity of smaller channels along the contour arc.

DISCUSSION

The commonly cited explanation for decreasing slope downfan as a result of grain-size fining is not consistent with data from the field sites that we have investigated (Fig. 17). Median bed-material grain sizes do not change detectably over large fractions of the channel length where slope declines, although sand fractions do increase downfan. In the case of fluvial transport, there are no established theories to predict channel gradient as a function of the largest grain size. So, most previous studies arguing for maximum grain-size control on fan slope (e.g., Blissenbach, 1952; Bluck, 1964; Denny, 1965; Kesel, 1985; Kesel and Lowe, 1987; Hubert and Filipov, 1989) cannot be interpreted using the available understanding of sediment transport. Observed patterns in bed-material grain size and sand fraction (Figs. 15 and 16) may also require some modifications to established models of fan sedimentology that depend on progressive grain-size fining downfan.

Drew's hypothesis that concave-up fan longprofiles result from progressive downfan deposition is consistent with calculations. Transport solutions for channel slopes require exponential gravel-deposition rates downfan. These rates result from the combination of rapid decline in hydraulic radius with a negligible change in median gravel-particle diameter and an expansion ratio and τ^*_{cr} reductions that are not sufficiently large to counteract the decline in τ^*. Even with this decline, flow depths far less than observed bankfull depths would be required to deposit bed material in-channel. Instead, observations of overbank deposition on low terraces or abandoned channels suggest that most deposition occurs where bed material moves overbank to cover older Active or Young alluvial deposits. This would explain the thin, late Holocene deposits (Fig. 14) observed in most channels. It would also be consistent with experiments by Sheets et al. (2002) showing that the majority of deposition occurs during short-duration,

TABLE 4. GAMMA SPECTROMETRY, COSMIC AND TOTAL DOSE RATES, AND EQUIVALENT DOSES AND AGES

Sample number	Sediment type[α]	K (%)	Th (ppm)	U (ppm)	Water content (%)	Cosmic dose rate (Gy/ka)[#]	Total dose rate (Gy/ka)[‡]	De (Gy)	n[ϕ]	Age (ka)
KS04-IV-33	Fluvial	3.76 ± 0.22	12.7 ± 0.37	1.43 ± 0.13	9.0 ± 0.4	0.18 ± 0.02	5.07 ± 0.13	28.0 ± 1.15[d]	7 (8)	5.52 ± 0.54
							7.66 ± 0.21	97.0 ± 1.07[e]	–	12.7 ± 0.72
								119 ± 0.80[e]	–	15.5 ± 0.83
KS05-IV-12	Eolian	3.56 ± 0.07	20.0 ± 0.40	2.06 ± 0.17	10 ± 0.5	0.23 ± 0.02	4.62 ± 0.08	> 231 ± 25.4[d]	13 (24)	> 50.1 ± 6.76
							6.10 ± 0.12	439 ± 32.9[e]	–	72.0 ± 4.14
								> 464 ± 58.0[e]	–	> 76.0 ± 6.17

[α]Discrete beds contained within the alluvial fan or wash
[#]Cosmic doses and attentuation with depth were calculated using the methods of Prescott and Hutton (1994)
[‡]Total dose rate is measured from moisture content of 10% as an average between field moisture and full saturation moisture values.
[d]Dose rate and age for fine-grained 250-105 um quartz sand using single-aliquot additive dose. Linear regression used on age, errors to one sigma
[e]Dose rate and age for fine-grained 4-11 um polymineral silt (IRSL) using multiple-aliquot additive dose. Exponential regression used on age, errors to one sigma. Correction for fading made using a g value of 5.27%/decade thus equivalent dose as given is original and not corrected
[ϕ]Number of replicated equivalent dose (De) estimates used to calculate the mean. Second number is total measurements made including failed runs with unusable data.

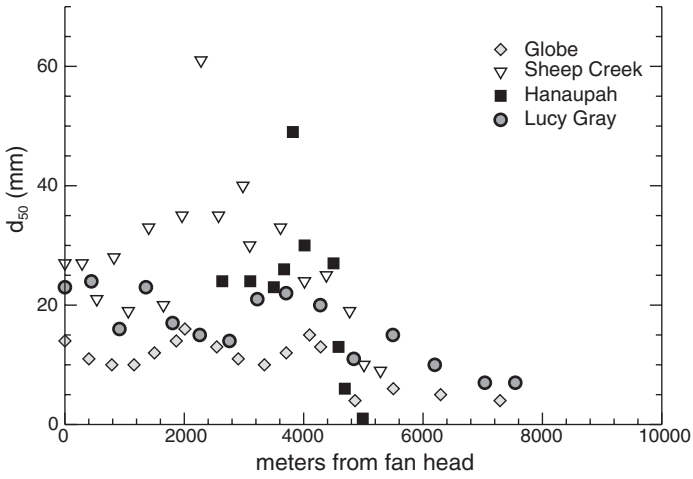

Figure 15. Plot of median gravel diameter versus distance from fan head. Resolvable fining occurs in the last ~25%–50% of the fan-channel lengths. Trends for 16th, 25th, 75th, and 84th percentiles are similar (Table 3).

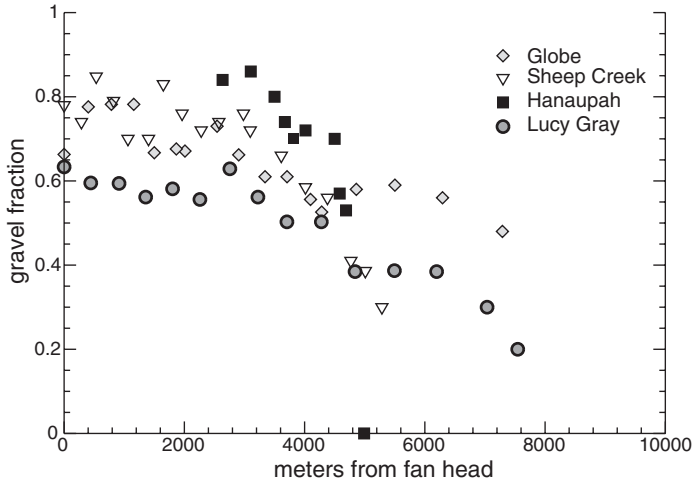

Figure 16. Plot of bed area gravel fraction versus distance from fan head.

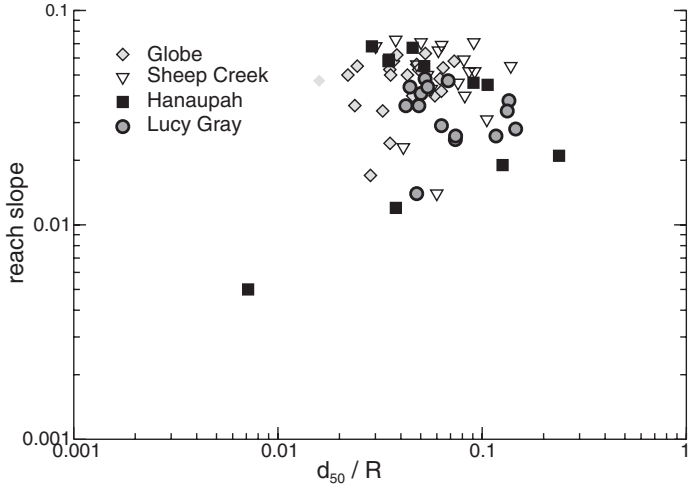

Figure 17. (A) Plot of reach slope against ratio of median grain size to hydraulic radius as a test of Shields' threshold explanation for fan-channel slope, assuming constant τ^*_c. Slopes of lines through each data set are indistinguishable from zero, indicating that these statements of the threshold channel are inconsistent with observed data on fans.

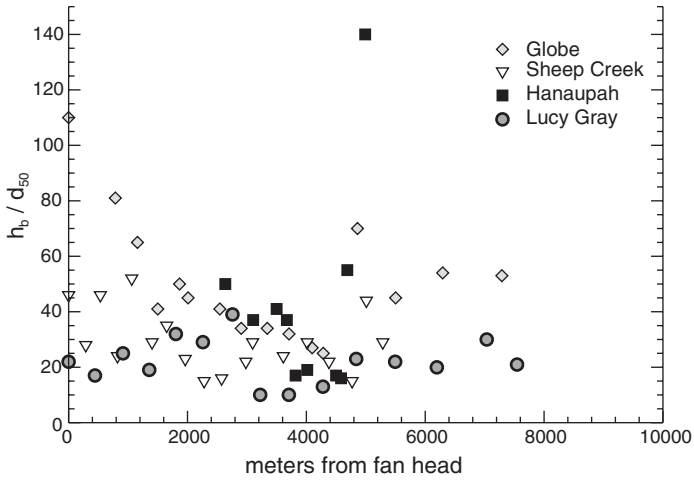

Figure 18. Plot of relative roughness (ratio of bankfull depth to median gravel diameter) versus distance from fan head, illustrating reduction in hydraulic radius.

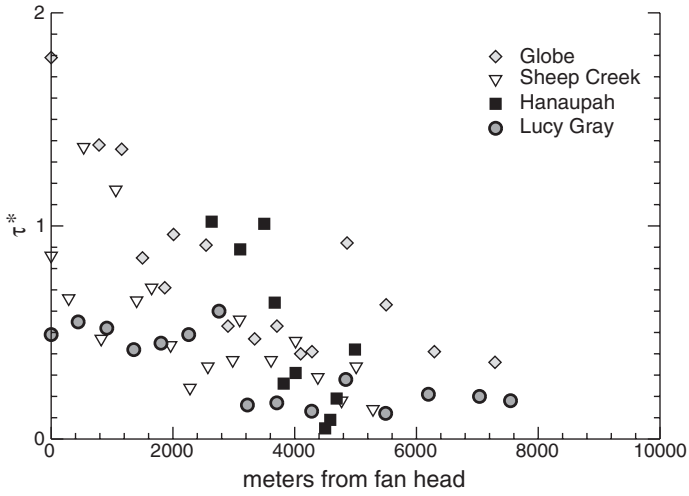

Figure 19. Plot of τ* versus distance from fan head, illustrating reduction in transport capacity downfan as hydraulic radius decreases.

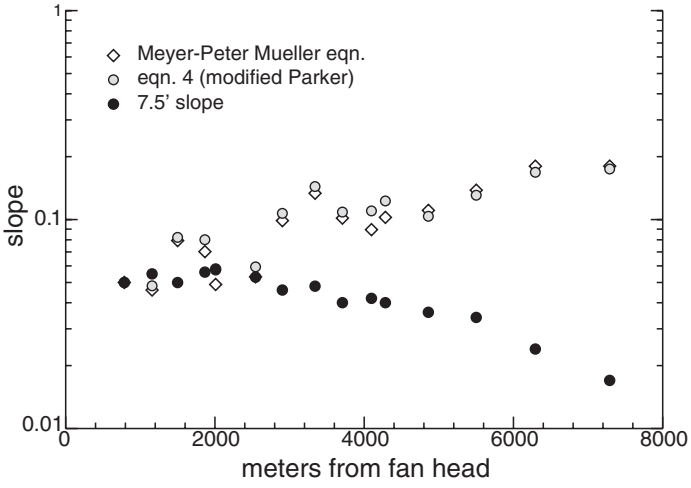

Figure 20. Plot of slope predicted by Equation (3) for Globe fan, assuming no gravel deposition downfan. MPM refers to Meyer-Peter and Mueller bedload equation (see Julien, 1998, equation 9.3a) is a common averaged shear stress bedload-transport equation. Increase in slope indicates that despite spreading of channels and reduction of t^*_c, substantial gravel deposition is required to match observed slopes with existing theory.

unchannelized flow. Field observations indicate three possible mechanisms for overbank, bed-material transport: (1) particle inertia ejection as the channel changes direction; (2) particle inertia ejection at in-channel obstructions like vegetation; and (3) local loss of banks leading to flow expansion and deposition. At present, we have no expectation about which process predominates on a given fan.

Field data from alluvial fans depart substantially from idealized parameters presented in Parker et al. (1998). Solutions for an idealized channelized fan in Parker et al. (1998) assume constant subsidence rates, flow depths that increase dramatically downfan as active channel widths decrease due to deposition, and constant Shields' stresses. The resulting long-profiles are largely statements about the planform geometry of the subsiding space to be filled and the increase in flow depth as sediment flux decreases downfan and channels narrow for a constant discharge. Field data from the fans in Figure 4 indicate that (1) Holocene subsidence rates are negligible; (2) hydraulic radius decreases downfan; (3) total active channel width is variable; and (4) Shields' stresses (τ*) decrease downfan. These differences require deposition of large gravel volumes downfan to match observed gradual slope reduction (e.g., Fig. 2). So, over timescales at which we can estimate bankfull depths from field data, Mojave fans depart significantly from published models. Over longer, Pleistocene timescales, higher terraces in Figure 7 do record aggradation at rates that decrease downfan, as recorded by decreasing elevations above modern channel floors. This pattern requires a model for variable downfan aggradation rates, missing at present because of a need for an overbank, bed-material deposition model.

At Holocene timescales, the declining hydraulic radius downfan is the most important influence on the transport calculations. Shallowing could result from any combination of (i) bifurcation of source catchment flow into distributary channels, (ii) transmission losses of water, or (iii) reductions in local runoff generation downfan. For instance, after storms in 2004 and 2005, surfaces where pedogenesis created strong Av or Bt horizons of low permeability produced minor runoff and sediment transport (Schmidt et al., 2004) that dissipated downfan. These observations raise the possibility that at least in the present climate, fan-channel runoff is locally sourced from older Pleistocene fan deposits, rather than from the source catchment. This may be one of the fundamental differences between temperate fans that depend on source catchment runoff and arid region fans with biologic soil crusts, silt-rich Av horizons, and impermeable subpavement B-horizons (e.g., Denny, 1965; Beaty, 1968) that can generate local Horton overland flow.

The interpretation of fan long-profiles as statements about sediment supply links the history of hillslope sediment production rates to fan surface slopes. For instance, surfaces of Pleistocene deposits (e.g., >72-ka sample from Fig. 5A) have higher slopes at Globe and adjacent fans (Fig. 22) than active channels. Test pits show that they also may have finer bed material. This combination is consistent with the hypothesis that the older, higher surface at Globe represents aggradation due to greater sediment supply. As an illustration, if the modern Globe channel had the slope of the Pleistocene deposit adjacent to it for the first seven cross sections (Fig. 22), its unit bedload flux from Equation (4) would be ~8% larger than that currently required to match its fan-head slope. Although one cannot rule out alternate hypotheses (e.g., wider channels and shallower flow at the same sediment supply) to explain the steeper slopes observed

on these older deposits, systematic increases in sediment supply from hillslopes in the past (e.g., Bull, 1991) might be a more testable hypothesis given current uses of cosmogenic radionuclides to estimate past lowering rates.

New views of the transport of the coarse size fractions (e.g., Solari and Parker, 2000) may also yield new interpretations of old observations. For instance, downfan decreases in maximum clast size observed in previous studies could reflect decreasing bankfull depths downfan. Field and flume experiments show that rapid flow over surfaces that are smooth relative to the maximum particle size can transport particles that approach, or even occasionally exceed flow depth (e.g., Fahnestock and Haushild, 1962; Fahnestock, 1963; Beaumont and Oberlander, 1971). This is probably a statement about the predominance of drag forces in steep channels with relatively low friction angles and fast, shallow flow (e.g., critical to supercritical flow in channels with substantial sand cover). Alluvial fan channels in parts of Death Valley transported large particles during 2004 rainfall events (e.g., Fig. 23), and previous observations indicate that channels on these fans can transport particles that approach and sometimes exceed flow depth at supercritical flow (Beaumont and Oberlander, 1971). In another instance, Stock observed flow and sediment transport over a small alluvial fan near Pescadero, California, in 2005. Shallow (<3-cm), rapid flow rolled waves of gravel down a flow thread, with particle tops often exposed above water as they rolled along a sandy bed. In this case, the combination of steep slope (~0.05), fast flow, and smooth channel-bed surface resulted in gravel moving at speeds that approached that of the fluid velocity. Particles accumulated behind inequant, slower rolling particles, and the sediment mass would move downstream until inertia would carry the mass of particles to deposit as a lobe overbank at a bend, or in an area of flow separation. If such conditions prevail widely during sediment transport on fans, particle inertia could play a strong role in off-channel gravel deposition at bends or in flow separation zones. Wasson (1974) speculated that this effect limited the movement of coarser particles downfan during flood surges in a steep Australian fan. It is clear that isolated boulders or groups of boulders downfan need not be interpreted solely as reworked debris-flow deposits.

Uncertainties in the transport calculations of this study illustrate opportunities to understand mechanics of steep-channel sediment transport during episodic flash floods. We are not aware of any field measurements of bedload flux during alluvial fan floods that could be used to validate using Equation (3). Nor is it clear that the techniques used by Wilcock and colleagues (Wilcock and McArdell, 1993; Wilcock et al., 2001; Wilcock and Kenworthy, 2002; Wilcock and Crowe, 2003) to reduce τ^*_c as sand fraction increases capture this effect under supercritical flow conditions on steep fan channels, where drag forces may predominate. We have also ignored the role of sediment and flow production on the fan, because of the difficulty in measuring it. A study by Griffiths et al. (2006) using impounded sediment to date overland flow events offers one innovative possibility to estimate at least the long-term fan runoff frequency. Together, these and other uncertainties mean that closing the problem on the control of alluvial fan slopes will require additional detailed studies of the hydraulics of fan channels, both in the laboratory and in the field.

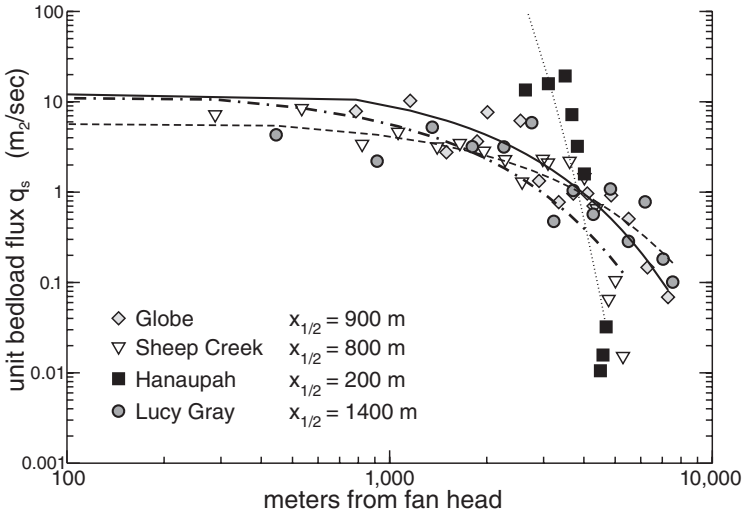

Figure 21. Plot of minimum required unit bedload flux at each cross section necessary to reproduce observed local slope. Downfan reductions can be characterized by exponential curves with the distance over which half the load is lost, varying from ~200 m for Hanupah to ~1400 m for Lucy Gray.

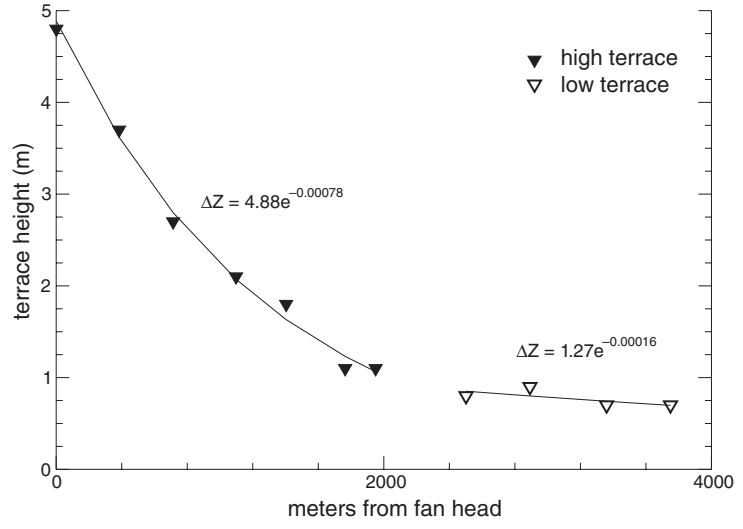

Figure 22. Height of older surfaces above current Globe mainstem channel (white line in Fig. 5), from 1-m LiDAR. Higher elevation and slope (+0.002) on these deposits is consistent with higher sediment supply at the time of their deposition. For modern bankfull depth and median grain size, this increased slope would require a unit sediment flux ~8% higher than the modern flux, sustained across the upper fan area.

Figure 23. View up road inundated by Desolation Canyon fan channel in 2004, Death Valley, California. A 0.6-m boulder (next to author) rests atop an old road surface, which slopes at 0.043; a trim line on the road berm to the left of this boulder indicates a maximum flow depth of 0.44 m. The image indicates that exceptionally large particles may be mobile on steep, finer grained fan channels where flow approaches maximum particle diameter. Observed decreases in maximum particle size down traction-dominated fans may be statements about decreasing flow depth.

CONCLUSION

We used field measurements of hydraulic geometry and granulometry on four alluvial fans in the arid American southwest to test two hypotheses to explain slopes of active alluvial fan channels. A lack of bedload fining down middle and upper fan channels, and the failure of Shields' criterion to explain observed reductions in these channel slopes, lead us to conclude that grain-size reduction alone does not control fan-channel long-profiles. Declining channel slopes downfan can be explained with reductions in transport rate downfan as gravel fractions deposit, a view first espoused by Drew in 1873. We find that with our current understanding of sediment transport, the bed-material deposition needed to reproduce observed fan-channel long-profiles can be approximated with an exponential decline in unit bedload flux downfan. The length scale over which half of the flux is deposited outside the channel varies from ~800–1400 m for three fans that are not cut by faults, and is significantly shorter (~200 m) for a fan cut by a normal fault that creates accommodation space for deposits. Much of this material appears to be deposited overbank in abandoned channels and low terraces. This finding highlights our lack of a mechanistic theory to predict rates of overbank, bed-material deposition. Predicted deposition rates downfan are also sensitive to details of sediment transport formula, and to an evolving understanding of the role that the abundance of relatively fine grain sizes plays in increasing transport rates.

ACKNOWLEDGMENTS

We thank Alison Duvall, Sarah Godfrey, Maiana Hanshaw, Leslie Hsu, Heather Lackey, Sarah Robinson, Johnny Sanders, and John Vogel for field assistance. Shannon Mahan did the luminescence sampling and dating. Stock thanks the U.S. Geological Survey Mendenhall Program and the Desert Southwest Surficial Mapping project for financial and logistical support. We thank Mark Reid, Michael Singer, Frank Pazzaglia, Terence Blair, and Dru Germanoski for their helpful reviews. Peter Wilcock generously provided the source data for Figure 10.

REFERENCES CITED

Albee, A.L., Labotka, T.C., Lanphere, M.A., and McDowell, S.D., 1981, Geologic map of the Telescope Peak Quadrangle, California, 1:62,500: U.S. Geological Survey Map GQ-1532.

Banerjee, D., Murray, A.S., Boetter-Jensen, L., and Lang, A., 2001, Equivalent dose estimation using a single aliquot of polymineral fine grains: Radiation Measurements, v. 33, no. 1, p. 73–94, doi: 10.1016/S1350-4487(00)00101-3.

Beaty, C.B., 1963, Origin of alluvial fans, White Mountains, California and Nevada: Annals of the Association of American Geographers: Association of American Geographers, v. 53, p. 516–535, doi: 10.1111/j.1467-8306.1963.tb00464.x.

Beaty, C.B., 1968, Sequential study of desert flooding in the White Mountains of California and Nevada: U.S. Army Natick Laboratories Technical Report 68-31-ES, 96 p.

Beaumont, P., 1972, Alluvial fans along the foothills of the Elburz Mountains, Iran: Palaeogeography, Palaeoclimatology, Palaeoecology, v. 12, p. 251–273, doi: 10.1016/0031-0182(72)90022-3.

Beaumont, P., and Oberlander, T.M., 1971, Observations on stream discharge and competence at Mosaic Canyon, Death Valley, California: Geological Society of America Bulletin, v. 82, p. 1695–1698, doi: 10.1130/0016-7606(1971)82[1695:OOSDAC]2.0.CO;2.

Bedford, D.R., Miller, D.M., Schmidt, K.M., and Phelps, G.A., 2007, Landscape-scale relationships between surficial geology, soil texture, topography, and creosote bush size and density in the Eastern Mojave Desert of California: *in* Webb, R.H., Fenstermaker, L.F., Heaton, J.S., Hughson, D.L., McDonald, E.V., and Miller, D.M., eds., The Mojave Desert: Ecosystem processes and sustainability, University of Nevada Press.

Blair, T.C., 1987, Sedimentary processes, vertical stratification sequences, and geomorphology of the Roaring River alluvial fan, Rocky Mountain National Park, Colorado: Journal of Sedimentary Petrology, v. 57, p. 1–18.

Blair, T.C., 1999, Cause of dominance by sheetflood vs. debris-flow processes on two adjoining alluvial fans, Death Valley, California: Sedimentology, v. 46, p. 1015–1028, doi: 10.1046/j.1365-3091.1999.00261.x.

Blair, T.C., 2000, Sedimentology and progressive tectonic unconformities of the sheetflood-dominated Hell's Gate alluvial fan, Death Valley, California: Sedimentary Geology, v. 132, p. 233–262, doi: 10.1016/S0037-0738(00)00010-5.

Blair, T.C., and McPherson, J.G., 1994a, Alluvial fans and their natural distinction from rivers based on morphology, hydraulic processes, sedimentary processes, and facies assemblages: Journal of Sedimentary Research, Section A, Sedimentary Petrology and Processes, v. 64, p. 450–489.

Blair, T.C., and McPherson, J.G., 1994b, Alluvial fan processes and forms, *in* Abrahams, A.D., and Parsons, A.J., eds., Geomorphology of desert environments: London, Chapman and Hall, p. 354–402.

Blissenbach, E., 1951, The geology of alluvial fans in Arizona [M.S. thesis]: University of Arizona, 86 p.

Blissenbach, E., 1952, Relation of surface angle distribution to particle size distribution on alluvial fans: Journal of Sedimentary Petrology, v. 22, no. 1, p. 25–28.

Blissenbach, E., 1954, Geology of alluvial fans in arid-regions: Geological Society of America Bulletin, v. 65, p. 175–190, doi: 10.1130/0016-7606(1954)65[175:GOAFIS]2.0.CO;2.

Bluck, B.J., 1964, Sedimentation of an alluvial fan in southern Nevada: Journal of Sedimentary Petrology, v. 34, p. 395–400.

Boothroyd, J.C., and Nummedal, D., 1978, Proglacial braided outwash: A model for humid alluvial fan deposits: Canadian Society of Petroleum Geologists, Memoir 5, p. 641–668.

Brady, R.H., 1986, Cenozoic geology of the northern Avawatz Mountains in relation to the intersection of the Garlock and Death Valley fault zones, San Bernardino County, California [Ph.D. thesis]: University of California, Davis, 292 p.

Bull, W.B., 1962, Relations of alluvial-fan size and slope to drainage-basin size and lithology in western Fresno County, California: U.S. Geological Survey Professional Paper 424-B, p. 51–53.

Bull, W.B., 1964a, Alluvial fans and near surface subsidence in western Fresno County, California: U.S. Geological Survey Professional Paper 437-A, p. A1–A71.

Bull, W.B., 1964b, Geomorphology of segmented alluvial fans in western Fresno County: U.S. Geological Survey Professional Paper 352-E, p. 89–129.

Bull, W.B., 1977, The alluvial fan environment: Progress in Physical Geography, v. 1, p. 222–270.

Bull, W.B., 1991, Geomorphic responses to climate change: New York, Oxford University, 326 p.

Chawner, W.D., 1935, Alluvial fan flooding, the Montrose, California, flood of 1934: Geographical Review, v. 25, p. 255–263, doi: 10.2307/209600.

Clarke, M.L., 1994, Infrared stimulated luminescence ages from aeolian sand and alluvial fan deposits from the eastern Mojave desert, California: Quaternary Geochronology, v. 13, p. 533–538.

Clayton, J.A., 1988, Quaternary tectonism of Sheep Creek alluvial fan deposits, Avawatz Mountains, southern Death Valley, *in* Gregory, J.L., and Baldwin, E.J., eds., Geology of Death Valley: South Coast Geological Society, p. 224–239.

Costa, J.E., 1984, Physical geomorphology of debris flows: *in* Costa, J.E., and Fleisher, P., eds., Developments and applications of geomorphology: Berlin, Springer-Verlag, p. 268–313.

Dawdy, D.R., 1979, Flood frequency estimates on alluvial fans: Journal of the Hydraulics Division, v. 105, HY11, p. 1407–1413.

Denny, C.S., 1965, Alluvial fans in the Death Valley region: U.S. Geological Survey Professional Paper 466, 62 p.

Denny, C.S., 1967, Fans and pediments: American Journal of Science, v. 265, p. 81–105.

Dorn, R.I., 1996, Climatic hypotheses of alluvial-fan evolution in Death Valley are not testable, *in* Rhoads, B.L., and Thorn, C.E., eds., The scientific nature of geomorphology: Proceedings of the 27th Binghamton Symposium in Geomorphology, p. 192–220.

Dorn, R.I., DeNiro, M.J., and Ajie, H.O., 1987, Isotopic evidence for climatic influence on alluvial-fan development in Death Valley, California: Geology, v. 15, p. 108–110, doi: 10.1130/0091-7613(1987)15<108:IEFCIO>2.0.CO;2.

Drew, F., 1873, Alluvial and lacustrine deposits and glacial records of the upper Indus basin: Quarterly Journal of the Geological Society of London, v. 29, p. 441–471.

Eckis, R., 1928, Alluvial fans of the Cucamonga district, southern California: The Journal of Geology, v. 36, p. 224–247.

Edwards, K.L., and Thielmann, J., 1984, Alluvial fans: Novel flood challenge: Civil Engineering, v. 11, p. 66–68.

Ethridge, F.G., 1985, Modern alluvial fans and deltas, *in* Flores, R.M., Ethridge, F.G., Miall, A.D., Galloway, W.E., and Fouch, T.D., eds., Recognition of fluvial depositional systems and their resource potential: Society for Sedimentary Geology, SEPM Short Course 19, p. 101–143.

Fahnestock, R.K., 1963, Morphology and hydrology of a glacial stream—White River, Mount Rainier Washington: U.S. Geological Survey Professional Paper 422-A, 70 p.

Fahnestock, R.K., and Haushild, W.L., 1962, Flume studies of the transport of pebbles and cobbles on a sand bed: Geological Society of America Bulletin, v. 73, p. 1431–1436, doi: 10.1130/0016-7606(1962)73[1431:FSOTTO]2.0.CO;2.

Field, J., 2001, Channel avulsion on alluvial fans in southern Arizona: Geomorphology, v. 37, p. 93–104, doi: 10.1016/S0169-555X(00)00064-7.

Forman, S.L., and Pierson, J., 2002, Late Pleistocene luminescence chronology of loess deposition in the Missouri and Mississippi river valleys, United States: Paleogeography, Paleoclimatolology, Paleoecology, v. 186, no. 1–2, p. 25–46, doi: 10.1016/S0031-0182(02)00440-6.

French, R.H., 1987, Hydraulic processes on alluvial fans: Amsterdam, Elsevier, 244 p.

French, R.H., and Lombardo, W.S., 1984, Assessment of flood hazard at the radioactive waste management site in area 5 of the Nevada Test Site: Water Resources Center, Desert Research Institute, University of Nevada.

Gile, L.H., Peterson, F.F., and Grossman, R.B., 1966, Morphological and genetic sequences of carbonate accumulation in desert soils: Soil Science, v. 101, p. 347–360, doi: 10.1097/00010694-196605000-00001.

Goldfarb, R.J., Miller, D.M., Simpson, R.W., Hoover, D.B., Moyle, P.R., Olson, J.E., and Gaps, R.S., 1988, Mineral resources of the Providence Mountains Wilderness Study Area, San Bernardino County, California: U.S. Geological Survey Bulletin 1712-D.

Griffiths, P.G., Hereford, R., and Webb, R.H., 2006, Sediment yield and runoff frequency of small drainage basins in the Mojave Desert, U.S.A: Geomorphology, v. 74, p. 232–244, doi: 10.1016/j.geomorph.2005.07.017.

Harvey, A.M., 1987, Alluvial fan dissection: Relationships between morphology and sedimentation, *in* Frostick, L.E, and Reid, I., eds., Desert sediments: Ancient and modern: Geological Society of London Special Publication 35, p. 87–103.

Harvey, A.M., 2002, The role of base-level change in the dissection of alluvial fans: Case studies from southeast Spain and Nevada: Geomorphology, v. 45, p. 67–87, doi: 10.1016/S0169-555X(01)00190-8.

Hewett, D.F., 1956, Geology and mineral resources of the Ivanpah quadrangle, California and Nevada: U.S. Geological Survey Professional Paper 275, 172 p.

Hooke, R.L.B., 1967, Processes on arid-region alluvial fans: The Journal of Geology, v. 75, p. 438–460.

Hooke, R.L.B., 1968, Steady-state relationships on arid-region alluvial fans in closed basins: American Journal of Science, v. 266, p. 609–629.

Hooke, R.L.B., 1972, Geomorphic evidence for late Wisconsin and Holocene tectonic deformation, Death Valley, California: Geological Society of America Bulletin, v. 83, p. 2073–2098, doi: 10.1130/0016-7606(1972)83[2073:GEFLAH]2.0.CO;2.

Hooke, R.L.B., and Dorn, R.I., 1992, Segmentation of alluvial fans in Death Valley, California: New insights from surface exposure dating and laboratory modeling: Earth Surface Processes and Landforms, v. 17, p. 557–574, doi: 10.1002/esp.3290170603.

Hooke, R.L.B., and Rohrer, W.L., 1977, Relative erodibility of source area rock types, as determined from second-order variations in alluvial-fan size: Geological Society of America Bulletin, v. 88, p. 1177–1182, doi: 10.1130/0016-7606(1977)88<1177:REOSRT>2.0.CO;2.

Hooke, R.L.B., and Rohrer, W.L., 1979, Geometry of alluvial fans: Effect of discharge and sediment size: Earth Surface Processes and Landforms, v. 4, p. 147–166.

Hubert, J.F., and Filipov, A.J., 1989, Debris-flow deposits in alluvial fans on the west flank of the White Mountains, Owens valley, California, U.S.A: Sedimentary Geology, v. 61, p. 177–205, doi: 10.1016/0037-0738(89)90057-2.

Hunt, C.B., and Mabey, D.R., 1966, Stratigraphy and structure, Death Valley, California: U.S. Geological Survey Professional Paper 494-A, 162p.

Ibbeken, H., Warnke, D.A., and Diepenbroek, M., 1998, Granulometric study of the Hanaupah fan, Death Valley, California: Earth Surface Processes and Landforms, v. 23, p. 481–492, doi: 10.1002/(SICI)1096-9837(199806)23:6<481::AID-ESP906>3.0.CO;2-T.

Ikeda, H., and Iseya, F., 1988, Experimental study of the heterogeneous sediment transport: Tsukuba: Environmental Research Center Paper, v. 12, p. 1–50.

Julien, P.Y., 1988, Erosion and Sedimentation: Cambridge, Cambridge University Press, 280 p.

Kesel, R.H., 1985, Alluvial fan systems in a wet-tropical environment, Costa Rica: National Geographic Research, v. 1, no. 4, p. 450–469.

Kesel, R.H., and Lowe, D.R., 1987, Geomorphology and sedimentology of the Toro Amarillo alluvial fan in a humid tropical environment, Costa Rica: Geografiska Annaler, Series A, v. 69, p. 85–99, doi: 10.2307/521369.

Kostaschuk, R.A., MacDonal, G.M., and Putnam, P.E., 1986, Depositional process and alluvial fan-drainage basin morphometric relationships near Banff, Alberta, Canada: Earth Surface Processes and Landforms, v. 11, p. 471–484, doi: 10.1002/esp.3290110502.

Lang, A., 1994, Infrared stimulated luminescence dating of Holocene reworked silty sediments: Quaternary Science Reviews, v. 13, no. 5–7, p. 525–528, doi: 10.1016/0277-3791(94)90071-X.

Lawson, A.C., 1913, The petrographic designation of alluvial fan formations: University of California Publications in Geological Sciences, v. 7, p. 325–334.

Lustig, L.K., 1965, Clastic sedimentation in Deep Springs Valley, California: U.S. Geological Survey Professional Paper 352-F, p. 131–192.

Machette, M.N., 1985, Calcic soils of the southwestern United States, *in* Weide, D.L., ed., Soils and Quaternary geology of the southwestern United States: Boulder, Colorado, Geological Society of America Special Paper 203, p. 1–21.

Mahan, S.A., Miller, D.M., Menges, C.M., and Yount, J.C., 2007, Late Quarternary stratigraphy and luminescence geochronology of the northeastern Mojave Desert, v. 166, p. 61–78.

Maher, K., Wooden, J.L., Paces, J.B., and Miller, D.M., 2007, ^{230}Th-U dating of surficial deposits using the ion microprobe (SHRIMP-RG): A microstratigraphic perspective: Quaternary International, v. 166, p. 15–28.

Major, J.J., and Iverson, R.M., 1998, Pebble orientation on large experimental debris-flow deposits: Sedimentary Geology, v. 117, p. 151–164, doi: 10.1016/S0037-0738(98)00014-1.

Marchi, L., Pasuto, A., and Tecca, P.R., 1993, Flow processes on alluvial fans in the Eastern Italian Alps: Zeitschrift fur Geomorphologie, v. 37, no. 4, p. 447–458.

Mather, A.E., and Hartley, A., 2005, Flow events on a hyper-arid alluvial fan: Quebrada Tambores, Salar de Atacama, northern Chile, *in* Harvey, A.M., Mather, A.E., and Stokes, M., eds., Alluvial fans: Geomorphology, sedimentology, dynamics: Geological Society of London Special Publication 251, p. 9–24.

McDonald, E.V., 1994, The relative influences of climatic change, desert dust, and lithologic control on soil-geomorphic processes and soil hydrology of calcic soils formed on Quaternary alluvial-fan deposits in the Mojave Desert, California [Ph.D. thesis]: University of New Mexico, 382 p.

McDonald, E.V., McFadden, L.D., and Wells, S.G., 2003, Regional response of alluvial fans to the Pleistocene-Holocene climatic transition, Mojave Desert, California: *in* Enzel, Y., Wells, S.G., and Lancaster, N., eds., Paleoenvironments and paleohydrology of the Mojave and southern Great Basin deserts: Boulder, Colorado, Geological Society of America Special Paper 368, p. 189–205.

McGowen, J.H., 1979, Alluvial fan systems, *in* Galloway, W.E., Kreitler, C.W., and McGowen, J.H., eds., Depositional and ground-water flow systems in the exploration for uranium in Austin, Texas: Bureau of Economic Geology, p. 43–79.

Melton, M.A., 1965, The geomorphic and paleoclimatic significance of alluvial deposits in southern Arizona: The Journal of Geology, v. 73, p. 1–38.

Miall, A.D., 1996, The geology of fluvial deposits: Sedimentary facies, basin analysis and petroleum geology: Berlin, Springer-Verlag, 582 p.

Millard, H.T., and Maat, P.B., 1994, Thermoluminescence dating procedures in use at the U.S. Geological Survey, Denver, Colorado: U.S. Geological Survey Open-File Report 94-249, 112 p.

Miller, D.M., Flint, A.L., Flint, L.E., Bedford, D.R., and Blainey, J.B., 2002, Mojave Desert soils and geomorphology: Implications for moisture budget for plants and susceptibility for erosion: Tucson, Arizona, 87th Annual Meeting of the Ecological Society of America and the 14th Annual International Conference of the Society for Ecological Restoration, August 4–9, 2002, p. 36.

Miller, D.M., Schmidt, K.M., Stock, J., Bedford, D.R., and Hughson, D.L., 2004, Contrasting summer and winter precipitation events and soil moisture response on a Mojave Desert alluvial fan: Redlands, California, Third Mojave Desert Science Symposium.

Miller, D.M., Bedford, D.R., Hughson, D.L., McDonald, E.V., Robinson, S.E., and Schmidt, K.M., 2007, Mapping Mojave Desert ecosystem properties with surficial geology, *in* Webb, R.H., Fenstermaker, L.F., Heaton, J.S., Hughson, D.L., McDonald, E.V., and Miller, D.M., eds., The Mojave Desert: Ecosystem processes and sustainability: Reno, Nevada, University of Nevada Press.

Mills, H.H., 2000, Controls on form, process, and sedimentology of alluvial fans in the Central and Southern Appalachians, southeastern U.S.A: Southeastern Geology, v. 39, p. 281–313.

Murray, A.S., and Wintle, A.G., 2000, Luminescence dating of quartz using an improved single-aliquot regenerative-dose protocol: Radiation Measurements, v. 32, no. 1, p. 57–73, doi: 10.1016/S1350-4487(99)00253-X.

Nilsen, T.H., 1982, Alluvial fan deposits, *in* Scholle, P.A., and Spearing, D., eds., Sandstone depositional environments: American Association of Petroleum Geologists Memoir, v. 31, p. 49–86.

Nimmo, J.R., Perkins, K.S., Winfield, K.A., Schmidt, K.M., Miller, D.M., Stock, J.D., and Singha, K., 2005, Field-measured infiltration properties of Mojave Desert soils with varying degrees of pedogenesis: Soil Science Society of America, Annual meeting, Abstract 266-1.

Parker, G., 1990, Surface-based bedload transport relation for gravel rivers: Journal of Hydraulic Research, v. 28, p. 417–436.

Parker, G., Paola, C., Whipple, K.X., and Mohrig, D., 1998a, Alluvial fans formed by channelized fluvial and sheet flow I. Theory: Journal of Hydraulic Engineering, v. 124, p. 985–995, doi: 10.1061/(ASCE)0733-9429(1998)124:10(985).

Parker, G., Paola, C., Whipple, K.X., Mohrig, D., Toro-Escobar, C.M., Halverson, M., and Skoglund, T.W., 1998b, Alluvial fans formed by channelized fluvial and sheet flow II. Application: Journal of Hydraulic Engineering, v. 124, p. 996–1004, doi: 10.1061/(ASCE)0733-9429(1998)124:10(996).

Pearthree, P.A., Klawon, J.E., and Lehman, T.W., 2004, Geomorphology and hydrology of an alluvial fan flood on Tiger Wash, Maricopa and La Paz Counties, west central Arizona: Arizona Geological Survey Open-File Report 04-02, 40 p.

Pelletier, J.D., Mayer, L., Pearthree, P.A., House, P.K., Demsey, K.A., Klawon, J.E., and Vincent. K.R., 2005, An integrated approach to flood hazard assessment on alluvial fans using numerical modeling, field mapping, and remote sensing: Geological Society of America Bulletin, v. 117, p. 1167–1180, doi: 10.1130/B25544.1.

Perkins, K.S., Nimmo, J.R., Winfield, K.A., Schmidt, K.S., Miller, D.M., and Stock, J.D., 2005, Field-measured infiltration properties of Mojave Desert soils: Eos (Transactions, American Geophysical Union), v. 86 (52), Fall Meeting Supplement, Abstract H21E–1394.

Peterson, F.F., 1981, Landforms of the Basin and Range Province defined for soil survey: Reno, Nevada, University of Nevada, Nevada Agricultural Experiment Station, p. 52.

Phelps, G.A., Robinson, S.E., and Miller, D.M., 2005, Investigating plant patterns on alluvial fan deposits of the Mojave Desert using high resolution imagery: Eos (Transactions, American Geophysical Union), v. 86 (52), Fall Meeting Supplement, Abstract B51D–0249.

Prescott, J.R., and Hutton, J.T., 1994, Cosmic-ray contributions to dose-rates for luminescence and ESR dating-large depths and long-term time variations: Radiation Measurements, v. 32, p. 57–73.

Price, W.E.J., 1974, Simulation of alluvial fan deposition by a random walk model: Water Resources Research, v. 10, no. 2, p. 263–274.

Rahn, P.H., 1967, Sheetfloods, streamfloods, and the formation of pediments: Annals of the Association of American Geographers. Association of American Geographers, v. 57, p. 593–604, doi: 10.1111/j.1467-8306.1967.tb00624.x.

Richardson, C.A., McDonald, E.V., and Busacca, A.J., 1997, Luminescence dating of loess from the northwest United States: Quaternary Science Reviews, v. 16, no. 3–5, p. 403–415, doi: 10.1016/S0277-3791(96)00111-4.

Ritter, J.B., Miller, J.R., Enzel, Y., Howes, S.D., Nadon, G., Grubb, N.D., Hoover, K.A., Olsen, T., Reneau, S.L., Sack, D., Summa, C.L., Taylor, I., Touysinhthiphonexay, K.N., Yodis, E.G., Schneider, N.P., Ritter, D.F., and Wells, S.G., 1993, Quaternary evolution of Cedar Creek alluvial fan, Montana: Geomorphology, v. 8, p. 287–304, doi: 10.1016/0169-555X(93)90025-W.

Roberts, H.M., and Wintle, A.G., 2001, Equivalent dose determinations for polymineralic fine-grains using the SAR protocol: Application to a Holocene sequence of the Chinese Loess Plateau: Quaternary Science Reviews, v. 20(5–9), p. 859–863.

Schmidt, K.M., and McMackin, M., 2006, Preliminary surficial geologic map of the Mesquite Lake 30' × 60' quadrangle, California and Nevada: U.S. Geological Survey Open-File Report 2006-1035, 89 p.

Schmidt, K.M., and Menges, C.M., 2003, Debris-flow deposits and watershed erosion rates near southern Death Valley, CA, United States, *in* Rickenmann, D., and Chen, C., eds., Debris-flow hazards mitigation: Mechanics, prediction, and assessment, Volume 1: Davos, Switzerland, Millpress, p. 219–230.

Schmidt, K.M., Nimmo, J., Miller, D., Stock, J., Winfield, K., Perkins, K., and Belknap, S., 2004, Quaternary geology, unsaturated soil-moisture measurements, and evidence for overland flow in the Globe Piedmont, Mojave Desert, CA: Eos (Transactions, American Geophysical Union), v. 85 (52), Fall Meeting Supplement, Abstract H31D–0420.

Sheets, B.A., Hickson, T.A., and Paola, C., 2002, Assembling the stratigraphic record: Depositional patterns and time-scales in an experimental alluvial basin: Basin Research, v. 14, p. 287–301, doi: 10.1046/j.1365-2117.2002.00185.x.

Singhvi, A.K., Sharma, Y.P., and Agrawal, D.P., 1982, Thermo-luminescence dating of sand dunes in Rajasthan, India: Nature, v. 295, no. 5847, p. 313–315, doi: 10.1038/295313a0.

Singhvi, A.K., Bluszcz, A., Bateman, M.D., and Rao, M.S., 2001, Luminescence dating of loess-palaeosol sequences and coversands: Methodological aspects and palaeoclimatic implications: Earth-Science Reviews, v. 54, no. l–3, p. l93–211, doi: l0.1016/S0012-8252(01)00048-4.

Sohn, M. F., Mahan, S. A., Knott, J. R., and Bowman, D. D., 2007, Luminescence ages for alluvial-fan deposits in southern Death Valley: Implications for climate-driven sedimentation along a tectonically active mountain front: Quarternary International, v. 166, p. 49–60.

Solari, L., and Parker, G., 2000, The curious case of mobility reversal in sediment mixtures: Journal of Hydraulic Engineering, v. 126, p. 185–197, doi: 10.1061/(ASCE)0733-9429(2000)126:3(185).

Sowers, J.M., Harden, J.W., Robinson, S.W., McFadden, L.D., Amundson, R.G., Jull, A.T., Reheis, M.C., Taylor, E.M., Szabo, B.J., Chadwick, O.A., and Ku, T.L., 1988, Geomorphology and pedology on the Kyle Canyon alluvial fan, southern Nevada, *in* Weide, D.L., and Faber, M.L., eds., This extended land: Geological journeys in the southern Basin and Range: University of Nevada, Department of Geosciences, p. 137–157.

Spencer, J.E., 1990, Geologic map of southern Avawatz Mountains, northeastern Mojave Desert region, San Bernardino county, California: U.S. Geological Survey Map MF-2117, 1:24,000.

Stock, J.D., and Dietrich, W.E., 2003, Valley incision by debris flows: Evidence of a topographic signature: Water Resources Research, v. 39, doi: 10.1029/2001WR001057.

Sylvester, A.G., 2001, Search for contemporaneous fault creep in Death Valley, 1970–2000, *in* Machette, M.N., Johnson, M.L., and Slate, J.L., eds., Quaternary and late Pliocene geology of the Death Valley region: Recent observations on tectonics, stratigraphy, and lake cycles, U.S. Geological Survey Open-File Report 01-51, p. N217–224.

Vincent, K.R., Pearthree, P.A., House, P.K., and Demsey, K.A., 2004, Inundation mapping and hydraulic reconstructions of an extreme alluvial fan flood, Wild Burro Wash, Pima County, southern Arizona: Arizona Geological Survey Open-File Report 04-04, 45 p., 1 plate and GIS data on disk.

Wang, Y., Amundson, R., and Trumbore, S., 1994, A model for soil $^{14}CO_2$ and its implications for using ^{14}C to date pedogenic carbonate: Geochimica et Cosmochimica Acta, v. 58, p. 393–399, doi: 10.1016/0016-7037(94)90472-3.

Wasson, R.J., 1974, Intersection point deposition on alluvial fans: An Australian example: Geografiska Annaler, Series A, v. 56, p. 83–92, doi: 10.2307/520429.

Wasson, R.J., 1977, Last-glacial alluvial fan sedimentation in the Lower Derwent Valley, Tasmania: Sedimentology, v. 24, p. 781–799, doi: 10.1111/j.1365-3091.1977.tb01915.x.

Wells, S.G., 1977, Geomorphic controls of alluvial fan deposition in the Sonoran Desert, southwestern Arizona, *in* Doerhing, D.O., ed., Geomorphology in arid regions: Binghamton, Proceedings 8th Annual Geomorphology Symposium, p. 27–50.

Wells, S.G., and McFadden, L.D., 1987, Comment on "Isotopic evidence for climatic influence on alluvial-fan development in Death Valley, California": Geology, v. 15, p. 1178, doi: 10.1130/0091-7613(1987)15<1178:CAROIE>2.0.CO;2.

Whipple, K.X, Parker, G., Paola, C., and Mohrig, D., 1998, Channel dynamics, sediment transport, and the slope of alluvial fans: Experimental study: The Journal of Geology, v. 106, p. 677–693.

Wilcock, P.R., and Crowe, J.C., 2003, Surface-based transport model for mixed-size sediment: Journal of Hydraulic Engineering, v. 129, p. 120–128, doi: 10.1061/(ASCE)0733-9429(2003)129:2(120).

Wilcock, P.R., and Kenworthy, S.T., 2002, A two-fraction model for the transport of sand/gravel mixtures: Water Resources Research, v. 38, no. 10, doi: 10.1029/2001WR000684.

Wilcock, P.R., and McArdell, B.W., 1993, Surface-based fractional transport rates: Mobilization thresholds and partial transport of a sand-gravel sediment: Water Resources Research, v. 29, p. 1297–1312, doi: 10.1029/92WR02748.

Wilcock, P.R., Kenworthy, S.T., and Crowe, J.C., 2001, Experimental study of the transport of mixed sand and gravel: Water Resources Research, v. 37, p. 3349–3358, doi: 10.1029/2001WR000683.

Williams, G.P., 1970, Flume width and water depth effects in sediment-transport experiments: U.S. Geological Survey Professional Paper 562-H, 37 p.

Yount, J.C., Schermer, E.R., Felger, T.J., Miller, D.M., and Stephens, K.A., 1994, Preliminary geologic map of Fort Irwin Basin, north-central Mojave Desert, California: U.S. Geological Survey Open-File Report 94-173, 1:24,000, 27 p.

Manuscript Received 21 February 2007
Revised Manuscript Received 17 July 2007
Manuscript Accepted 31 July 2007

Printed in the USA